



# Hydrogel interfaces for merging humans and machines

Hyunwoo Yuk<sup>1,3</sup>✉, Jingjing Wu<sup>1</sup> and Xuanhe Zhao<sup>1,2</sup>✉

**Abstract** | The last few decades have witnessed unprecedented convergence between humans and machines that closely operate around the human body. Despite these advances, traditional machines made of hard, dry and abiotic materials are substantially dissimilar to soft, wet and living biological tissues. This dissimilarity results in severe limitations for long-term, reliable and highly efficient interfacing between humans and machines. To bridge this gap, hydrogels have emerged as an ideal material candidate for interfacing between humans and machines owing to their mechanical and chemical similarities to biological tissues and the versatility and flexibility in designing their properties. In this Review, we provide a comprehensive summary of functional modes, design principles, and current and future applications for hydrogel interfaces towards merging humans and machines.

## Capacitance

$C=q/V$ , where  $q$  is the charge held on the conductor and  $V$  is the electric potential of the conductor. Unit: F.

In the last century, advances in the understanding and engineering of the human body were made possible through interdisciplinary efforts in modern medicine, biology and biomedical engineering. In parallel, complex and ever more capable machines, such as computers, mobile devices, sensors, actuators and robots, have transitioned from science fiction into daily realities. Despite these advances, artificial interfaces — facilitating communication and interactions between humans and machines — are still largely primitive, leading to short-term and inefficient interfacing between humans and machines. These shortcomings are especially apparent in the emerging fields of brain–machine interfaces, neuroprosthetics, clinical equipment, medical implants, wearable and ingestible devices, and virtual or augmented reality. Long-term, efficient, biocompatible and seamless communication and interactions between humans and machines could lead to breakthroughs in these emerging sectors and other technological fields but have not been achieved due to lingering challenges. For example, conventional probes and arrays used for brain–machine interfaces and neuroscientific studies, such as the Michigan probes and Utah arrays, commonly induce substantial foreign-body responses, such as gliosis and scar formation, severely hampering the long-term reliability and functionality of brain–machine interfaces<sup>1–6</sup>. As another example, implantable glucose sensors and insulin pumps for diabetic monitoring and management often face substantially limited efficacy in the long term owing to fibrotic encapsulation induced by a foreign-body response and subsequent loss of the functional interfaces for sensing and delivery to the surrounding tissues<sup>7–12</sup>.

The main challenges of human–machine interfaces stem from materials. Existing machines largely employ conventional materials, such as metals, silicon, glass, ceramics and plastics, to communicate and interact with human bodies. However, the hard, dry and abiotic nature of these conventional materials is intrinsically contradictory with the soft, wet and living nature of biological tissues. In recent decades, intensive efforts have been devoted to transforming these conventional materials into flexible and stretchable structures to conformally interface with soft and curvilinear biological tissues<sup>1,13–17</sup>. However, these structural designs do not alter the materials' intrinsic properties, which may still hamper their communication and interactions with biological tissues. For example, the integration of conventional materials with tissues usually relies on physical attachment or surgical suturing, methods that face challenges such as non-conformal contact, unstable adhesion, tissue damage and/or scar formation<sup>15,18,19</sup>. As another example, the properties of metallic electrodes, such as their high rigidity, low interfacial capacitance and low charge injection capacity, make them far from ideal for the electrical recording and stimulation of soft neural tissues<sup>1,2,5,17,20–22</sup>. In addition, biological tissues often recognize these materials, even when in flexible and stretchable structures, as foreign bodies due to their inherently disparate properties, resulting in an adverse foreign-body response, biofouling, and fibrotic encapsulation or fibrosis<sup>2,23,24</sup>. Such foreign-body response and subsequent fibrotic isolation from the surrounding tissues can severely compromise the long-term reliability and efficacy of the communication and interactions between humans and machines<sup>10,23,25–29</sup>.

<sup>1</sup>Department of Mechanical Engineering, Massachusetts Institute of Technology, Cambridge, MA, USA.

<sup>2</sup>Department of Civil and Environmental Engineering, Massachusetts Institute of Technology, Cambridge, MA, USA.

<sup>3</sup>Present address: SanaHeal, Inc., Cambridge, MA, USA.

✉e-mail: [hyunwoo@mit.edu](mailto:hyunwoo@mit.edu); [zhaox@mit.edu](mailto:zhaox@mit.edu)

<https://doi.org/10.1038/s41578-022-00483-4>

Box 1 | Similarities between hydrogels and biological tissues

**High water content**

The human body contains few organs with a relatively low water content (such as bone, ~25% of weight) and many organs with a high water content (such as muscle, ~70% of weight, and brain, ~85% of weight), resulting in an average water content of ~70% of body weight<sup>270</sup> (see the figure, part a). By contrast, most engineering materials, such as silicon, metals, ceramics, plastics and elastomers, are dry and contain little or no water<sup>5</sup>. Because water in biological tissues serves critical roles in diverse biological, chemical and physical processes, including nutrient and waste transportation, intercellular signalling by waterborne chemicals, and ionic electrophysiological communication, hydrogels with a tissue-like high water content can closely mimic physiological interactions and minimize potential issues caused by dry foreign materials.

**Mechanical softness**

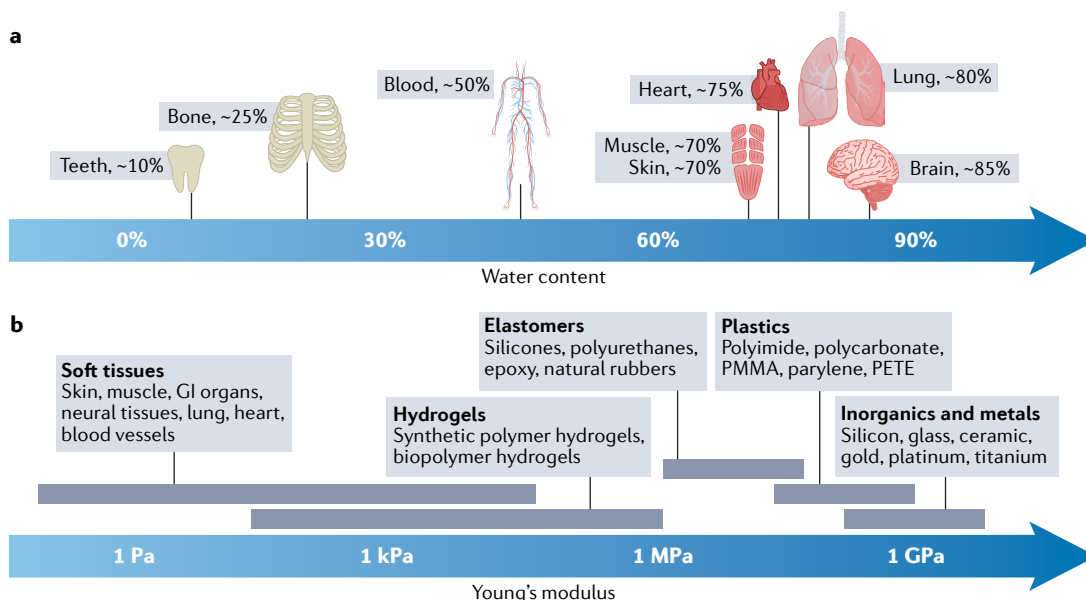
The human body is largely composed of soft tissues with few exceptions such as teeth and bone. Soft tissues in the human body have Young's moduli typically in the range of 1 Pa to 1 MPa, whereas most conventional solids, such as elastomers, plastics, inorganics and metals, exhibit Young's moduli several orders of magnitude higher<sup>2,13</sup> (see the figure, part b). This stark difference in mechanical properties is one of the major sources of tissue damage, foreign-body response and scar tissue formation around the rigid devices interfacing with the human body<sup>1-3,5</sup>. By contrast, hydrogels can have Young's moduli similar to those of biological tissues owing to their structural and compositional similarities as highly hydrated polymer networks.

**Biocompatibility**

Biocompatibility is one of the most crucial requirements for interfacing with the human body while avoiding adverse biological interactions and outcomes. Owing to their non-toxic and biocompatible nature, hydrogels have been widely studied and adopted in tissue engineering<sup>31</sup>, regenerative medicine<sup>29,32</sup> and biomedical devices<sup>41</sup> in both academic research and commercial products. Furthermore, hydrogels can offer antifouling<sup>64,66-68</sup> functions and reduce foreign-body responses<sup>69-78</sup> when in contact with physiological environments.

**Biofunctionality**

Both biological tissues and hydrogels are water-based polymer systems, and a broad range of biopolymers and synthetic polymers with biologically important functional groups can be used as constituents for hydrogels<sup>31,33,80,81</sup>. For example, various extracellular matrix components (such as collagen, gelatin and hyaluronic acid) as well as chemically modified biopolymers and synthetic polymers (such as arginyl-glycyl-aspartic acid (RGD) peptide-modified alginate and polyethylene glycol) have been adopted in hydrogels to facilitate biological functionalities (such as cell adhesion<sup>253</sup> and tissue engineering<sup>29,31</sup>).



GI, gastrointestinal; PMMA, poly(methyl methacrylate); PETE, poly(ethylene terephthalate).

Because of their unique similarities to biological tissues<sup>30-33</sup> (BOX 1) and the versatility and flexibility in tailoring their properties<sup>5,33-37</sup>, hydrogels have naturally emerged as a promising material candidate to act as an alternative or adjunct to conventional materials for bridging humans and machines. Hydrogel interfaces — both explored in academic research and as commercial products — are rapidly emerging in a broad range of applications (FIG. 1). For instance, ultrasound-coupling

hydrogels have been commercialized and have become the standard interfaces between ultrasound equipment and human skin for various medical imaging and therapeutic applications<sup>37-42</sup>. Similarly, commercially available skin-adhesive hydrogels have become the main candidates for epidermal electrodes used in clinical bioelectronic recordings, such as in electrocardiography, electromyography (EMG) and electroencephalography, and in clinical bioelectronic stimulation such as

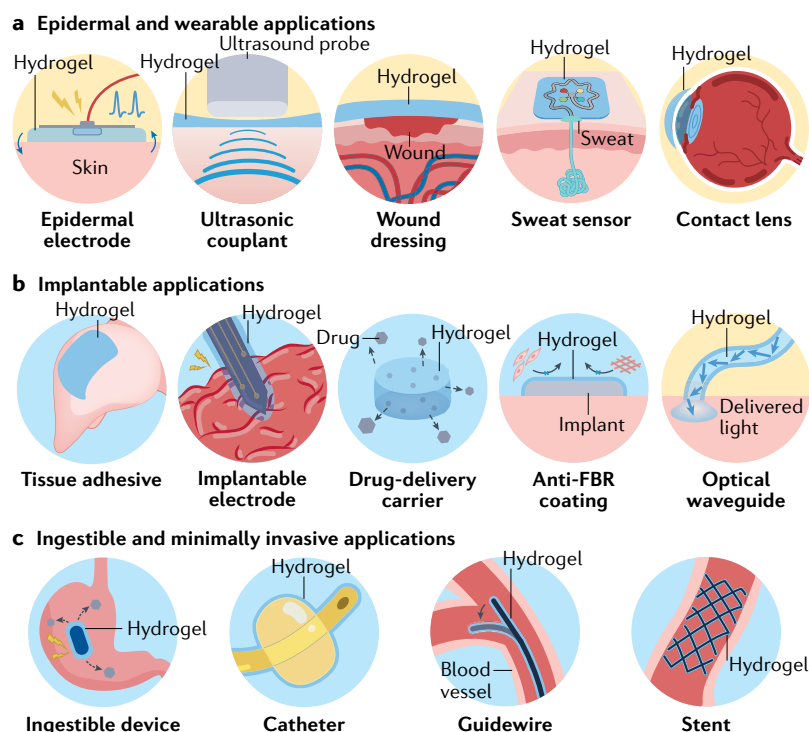


Fig. 1 | **Current applications of hydrogel interfaces.** Various examples of hydrogel interfaces for epidermal and wearable (part a), implantable (part b), and ingestible and minimally invasive (part c) applications around the human body. FBR, foreign-body response.

transcutaneous electrical nerve stimulation<sup>5,41–45</sup>. Besides their application as ultrasound-coupling agents and bioelectrodes, hydrogels have also been intensively explored as sensors, actuators and drug reservoirs in wearable devices such as sweat sensors<sup>16–48</sup>, contact lenses<sup>49–52</sup>, and wound dressings and bandages<sup>53–56</sup>. In addition, taking advantage of their edible, food-like properties and tunable swelling and degradation properties, hydrogels have recently emerged as a promising carrier for ingestible sensors and devices capable of long-term retention and functions in the gastrointestinal tract<sup>57–59</sup>. Furthermore, hydrogels with designed mechanical properties and chemical compositions have been shown to substantially enhance the biocompatibility of implantable devices by providing highly lubricious surfaces<sup>60–65</sup>, reducing biofouling<sup>64,66–68</sup> and alleviating foreign-body responses<sup>69–78</sup>. This enhanced biocompatibility paves the way for various implantable devices to form long-term reliable and functional interfaces with the human body.

Despite the great promise and recent advances in hydrogel interfaces, to the best of our knowledge, there is no systematic discussion on hydrogel interfaces for the merging of humans and machines. The literature on hydrogels as scaffolds for tissue engineering<sup>31,32,79–83</sup>, carriers for drug delivery<sup>84–87</sup> and emerging materials for soft machines<sup>34,88</sup> has been extensively reviewed, but existing reviews usually do not account for the applications of hydrogels as bridging interfaces between humans and machines nor do they provide the requirements or principles for the design of hydrogel interfaces. Such a systematic discussion is central for the future development of this nascent yet impactful field.

In this Review, we first provide a comprehensive summary of recent advances in hydrogel interfaces using examples from both academic literature and commercial products. Based on the nature of the communication and interactions between humans and machines, the functions of hydrogel interfaces can be broadly categorized into mechanical, acoustic, electrical, optical, chemical and biological modes. Thereafter, we systematically discuss the property requirements for hydrogel interfaces to enable various functional modes and provide the design principles to achieve such properties. We conclude with future perspectives on next-generation hydrogel interfaces and the remaining challenges and opportunities.

### Applications of hydrogel interfaces

Along with various devices and machines in contact and interacting with human bodies, hydrogel interfaces have emerged and have been adopted in diverse applications in both academic and commercial settings (TABLE 1). The current applications of hydrogel interfaces can be largely categorized based on the invasiveness of their interactions with various parts of the human body (FIG. 1). Hydrogel interfaces for epidermal and wearable applications (FIG. 1a) provide non-invasive communication, whereas hydrogel interfaces for implantable applications (FIG. 1b) are invasive and often provide long-term contact with internal organs and tissues. Hydrogel interfaces are also increasingly adopted in ingestible and minimally invasive applications within body cavities (such as thoracic and abdominal cavities) or tubular organs (such as intestines and blood vessels) (FIG. 1c). In this section, we review current applications of hydrogel interfaces from each category using examples from the literature and commercially available products (TABLES 1 and 2).

**Epidermal and wearable applications.** Skin is the largest organ in the human body and forms the body's outermost interface to external environments<sup>15</sup>. The facile and non-invasive nature of epidermal interfacing has encouraged the development of a wide range of epidermal and wearable devices, many of which have been commercialized and adopted as the standard of care in clinical practice. Despite its environment-exposed nature, skin possesses starkly different properties than conventional materials used in devices and machines. To bridge these dissimilarities and allow stable functionality, diverse hydrogel interfaces have been adopted in epidermal and wearable applications (FIG. 1a).

Epidermal electrodes are an essential component for various electrical sensing and stimulation devices in health monitoring<sup>15</sup>, diagnostic<sup>5,15</sup>, therapeutic<sup>45,89</sup> and human-machine interfacing<sup>90</sup> applications. The efficacy of epidermal electrical communications is influenced by several factors, including conformal mechanical contact with skin and the degree of skin hydration<sup>5,43,91</sup>. Conventional metallic electrodes are dry and mechanically stiff; therefore, they face various limitations, such as poor interfacial contact with dehydrated skin tissues, resulting in high skin-electrode interfacial impedance and ineffective electrical communication<sup>5</sup>. To address these limitations, hydrogel interfaces were introduced as coatings on metal electrodes and have become the standard

Table 1 | Current applications, functional modes and translation statuses of hydrogel interfaces

Applications	Examples	Functional mode	Translation status	Refs.
Epidermal and wearable applications	Epidermal hydrogel electrodes	Mechanical, electrical	Academic and commercial	5,15,45,89,157
	Hydrogel wound dressing	Mechanical, chemical, biological	Academic and commercial	53–56,99
	Hydrogel drug-delivery patch	Mechanical, chemical, biological	Academic and commercial	53,97,98
	Hydrogel ultrasound couplants	Mechanical, acoustic	Academic and commercial	38,93,94,170
	Hydrogel contact lenses	Mechanical, optical	Academic and commercial	49–52,108–110
	Hydrogel glucose sensors	Electrical, optical, chemical	Academic	262,263
	Hydrogel pH sensors	Electrical, chemical	Academic	54
Implantable applications	Tissue adhesives and sealants	Mechanical, chemical, biological	Academic and commercial	113–117,264
	Hydrogel electrode coatings	Mechanical, electrical	Academic	5,76–78
	Hydrogel waveguides	Mechanical, optical	Academic	110,141–144
	Drug-eluting hydrogels	Chemical, biological	Academic and commercial	42,84–87,167
	Tissue scaffolds	Chemical, biological	Academic and commercial	29,31,259,265
	Hydrogel glucose sensors	Chemical, biological	Academic	266,267
	Anti-FBR hydrogel coatings	Mechanical, biological	Academic	64,66–68,147
Ingestible and minimally invasive applications	Ingestible hydrogels for drug delivery or sensing	Mechanical, chemical, biological	Academic	57–59
	Ingestible hydrogels for weight control	Mechanical, chemical, biological	Academic and commercial	58,150,268
	Low-friction hydrogel coatings for minimally invasive devices	Mechanical, biological	Academic and commercial	64,151–154

FBR, foreign-body response.

electrode coatings in various clinical diagnostic (such as electrocardiography, electromyography and electroencephalography) and therapeutic (such as transcutaneous electrical nerve stimulation) applications. The soft and adhesive properties of hydrogel epidermal electrodes provide conformal contact with skin, and their high water content and high electrical conductivity offer low tissue–electrode impedance, synergistically leading to effective electrical sensing and stimulation. Notably, the majority of commercially available and clinically approved epidermal electrodes are composed of ionic hydrogel interfaces consisting of crosslinked hydrophilic polymers, such as polyacrylate copolymers, which have a high water content, good skin adhesiveness and dissolved ions (for example, potassium chloride) for electrical conductivity<sup>5,92</sup> (TABLE 2).

Furthermore, epidermal diagnostic imaging techniques, such as ultrasonography, rely on hydrogel couplants at the tissue–ultrasound probe interface, owing to the tissue-like mechanical and acoustic characteristics of hydrogels<sup>38,93–96</sup>. Hydrogel interfaces have also been widely adopted for the treatment of injured skin in the form of wound dressings or epidermal bandages owing to their unique capabilities for promoting wound healing through dehydration prevention, antimicrobial protection and transdermal drug delivery<sup>53,55,56,97–99</sup> (TABLE 2). In addition, hydrogel interfaces have been used in many epidermal health monitoring and diagnostic applications<sup>100</sup>. For example, the high water absorption of various chemical-sensing hydrogels enables their use as diagnostic devices based on epidermally collected body fluids such as sweat<sup>45,101–107</sup>.

Beyond skin, hydrogel interfaces have been widely utilized in ophthalmic wearable devices to interface with the eye. The soft, wet and transparent nature of hydrogels and their optical properties, such as their tunable refractive index, are highly desirable for ophthalmic interfacing. The majority of contact lenses, including clinically approved products based on poly(2-hydroxyethyl methacrylate) (Acuvue, J&J) and polyvinyl alcohol hydrogels (Dailies, CIBA Vision) (TABLE 2), have been based on hydrogels since the first commercial launch of hydrogel-based soft contact lenses in the 1970s<sup>108,109</sup>. More recently, various health monitoring and diagnostic functions have been introduced to ophthalmic hydrogel interfaces to create smart contact lenses<sup>49–52,108,110</sup>.

**Implantable applications.** In order for devices or machines to interface over the long term with internal tissues and organs, they often need to be implanted into the human body. Unlike non-invasive epidermal interfacing, implantable applications involve invasive surgical procedures and introduction of foreign objects within the human body. As a result, implantable applications face various challenges, including tissue damage, foreign-body responses and subsequent functional failure of the implants. These challenges often originate from and are substantially exacerbated by disparate properties between biological tissues and the implants. Hydrogel interfaces have been adopted for diverse implantable applications to resolve or alleviate these challenges (FIG. 1b).

**Electrical conductivity**

For an ideal conductor, the electrical conductivity is  $\sigma = L / RA$ , where  $L$  is the length,  $A$  is the cross-sectional area and  $R$  is the electrical resistance of the material. The reciprocal of electrical conductivity is electrical resistivity. Unit:  $\text{Sm}^{-1}$ .

**Refractive index**

$n = c/v$ , where  $c$  is the speed of light in a vacuum and  $v$  is the speed of light in the material. Unitless.

**Charge injection capacity**

Amount of charge that the electrode can inject per unit area without causing irreversible electrochemical reactions or tissue damage.

**Young's modulus**

The Young's modulus of a material in the linear elastic region is  $E=S/\epsilon$ , where  $S$  is the engineering stress and  $\epsilon$  is the engineering strain of the material. Unit: Pa.

The surgical repair of injured tissues and implantation of devices on targeted organs commonly requires establishing robust mechanical interfaces between the injured tissues and between the devices and organs, respectively. Conventional techniques to form mechanical interfaces, such as sealing and fixation, rely on sutures and surgical staples<sup>111</sup>. However, sutures and surgical staples commonly damage tissues, and their substantial mismatch with tissue properties can cause various adverse outcomes and complications, including scar formation, impaired healing and leakages<sup>112</sup>. In recent decades, tissue adhesives and sealants have been developed to address the limitations of sutures and surgical staples<sup>113–115</sup>. Because hydrogels provide robust, biocompatible and tissue-matching adhesive interfaces, a broad range of hydrogels based on synthetic polymers<sup>116,117</sup> (such as polyethylene glycol) and biopolymers<sup>118,119</sup> (such as fibrin or gelatin) have been adopted in implantable tissue adhesives for tissue repair<sup>114</sup> and integrated in devices both in academic studies and in clinically approved products<sup>19</sup> (TABLE 2).

Implantable electrodes for neurological treatment (such as deep brain stimulation)<sup>120–122</sup>, for rehabilitation (such as spinal cord stimulation)<sup>123–127</sup> and for functional augmentation involving, for example, pacemakers<sup>128–131</sup>, cochlear implants<sup>132</sup> or neuroprosthetics<sup>2,133–135</sup>, require

reliable bioelectronic communication and modulation over extended periods of time. However, conventional metallic implantable electrodes can elicit adverse responses such as fibrosis and scar formation from the target and surrounding tissues, resulting in functional loss owing to a decrease in signal-to-noise ratios during recording and a decrease in charge injection capacity during stimulation<sup>2,4,6,21</sup>. To address these issues, hydrogel interfaces have been introduced as adjunct or alternatives to metallic electrodes to provide improved biocompatibility<sup>69,76,136,137</sup> due to their tissue-matching Young's modulus and lower bending stiffness as well as improved electrical properties<sup>5,77,78,138,139</sup> resulting from their lower impedance and higher charge injection capacity.

Optical interfacing has also been utilized in implantable applications for photomedicine in photothermal therapy, photodynamic therapy and photobiomodulation<sup>110</sup> as well as for the modulation of neural activities in optogenetics<sup>21,140</sup>, where optical communication with the target tissue commonly relies on implanted waveguides<sup>110</sup>. However, conventional optical waveguides are made of silica or plastics and their mechanical mismatch with biological tissues can cause various adverse outcomes and deterioration of functionalities<sup>110</sup>. To avoid these limitations, hydrogel-based implantable optical waveguides with tissue-matching mechanical

**Table 2 | A representative list of clinically approved materials for hydrogel interfaces**

Hydrogel material	Product/company	Application	Approved indication
<b>Epidermal and wearable applications</b>			
Polyacrylate copolymer (with dissolved potassium chloride)	Red Dot/3M	Hydrogel skin electrodes	Electrocardiograph electrodes (FDA approved)
Polyacrylate copolymer (with dissolved potassium chloride)	Self-Adhesive Electrodes/Philips	Hydrogel skin electrodes	Cutaneous electrodes for TENS (FDA approved)
Polyethylene glycol	Aquaflor/Covidien	Hydrogel wound dressings	Wound dressings for first- and second-degree burns (FDA approved)
Polyacrylic acid	Aquasonic/Parker Laboratories	Hydrogel ultrasound couplants	Coupling medium for ultrasound transmission (FDA approved)
Poly(2-hydroxyethyl methacrylate)	Acuvue/J&J	Hydrogel contact lenses	Daily wear contact lens (FDA approved)
Polyvinyl alcohol	Dailies/CIBA Vision	Hydrogel contact lenses	Daily wear contact lens (FDA approved)
<b>Implantable applications</b>			
Polyethylene glycol	CoSeal/Baxter	Tissue adhesives	Adjunct haemostasis for vascular reconstitution (FDA approved)
Fibrin	Evicel/J&J	Tissue adhesives	Adjunct haemostasis (FDA approved)
Gelatin	LifeSeal/LifeBond	Tissue adhesives	Staple-line reinforcement in gastrointestinal surgery (CE marked)
Poly(2-hydroxyethyl methacrylate)	Vantas/Endo Pharmaceuticals	Drug-eluting hydrogels	Palliative treatment of prostate cancer (FDA approved)
Hyaluronic acid	Euflexxa/Ferring Pharmaceuticals	Tissue scaffolds	Knee osteoarthritis (FDA approved)
Alginate	Algisyl-LVR/LoneStar Heart	Tissue scaffolds	Advanced heart failure (CE marked)
<b>Ingestible and minimally invasive applications</b>			
Cellulose	Plenty/Gelesis	Ingestible hydrogels	Ingestible hydrogels to aid in weight management (FDA approved)
Polyvinylpyrrolidone	SpeediCath/Coloplast	Low-friction hydrogel coatings	Urinary catheters (FDA approved)
Poly(methyl vinyl ether/maleic anhydride)	Radifocus/Terumo Corporation	Low-friction hydrogel coatings	Cardiovascular guidewires (FDA approved)
	Vortek/Coloplast	Low-friction hydrogel coatings	Ureteral stents (FDA approved)

Date of search: December 2021. CE, Conformité Européenne (European Conformity); TENS, transcutaneous electrical nerve stimulation.



properties have been developed as a promising alternative to conventional stiff optical waveguides<sup>110,141–144</sup>.

Sustained delivery of pharmacological substances from implanted reservoirs is one of the major strategies for the treatment of various diseases<sup>145</sup>. Hydrogels have played an important role in the development and translation of implantable drug delivery systems owing to their favourable characteristics, including high water content, ease of chemical modification and incorporation of drugs, biocompatibility, and biodegradability<sup>84,87,146</sup>. As a result, various hydrogels, such as poly(2-hydroxyethyl methacrylate), hyaluronic acid and alginate, have been adopted in clinically approved products as implantable drug reservoirs or tissue scaffolds<sup>31,42,87</sup> (TABLE 2). In implantable applications, such as for sustained drug delivery, the foreign-body response and subsequent blockage of drug release by biofouling and fibrosis around the implanted devices is a critical issue hampering long-term efficacy<sup>9</sup>. To alleviate this challenge, diverse anti-foreign-body response hydrogel interfaces have been adopted in implantable machines and devices in academic studies to minimize the formation of fibrotic encapsulation (by reducing protein absorption and inflammatory reactions) and to preserve long-term functional efficacy<sup>64,66–68,147</sup>.

**Minimally invasive applications.** Interfacing within body cavities, such as abdominal and thoracic cavities, and tubular organs, such as the intestines, blood vessels and the urinary tract, provides minimally invasive yet close interactions with the human body. Orally administered ingestible devices have been developed for diverse diagnostic and therapeutic gastrointestinal applications<sup>49</sup>. Recent advances in endoscopic and robot-assisted surgical platforms have enabled a rapid growth in minimally invasive and robotic surgeries<sup>148</sup>. Despite the minimally invasive nature of these applications, close interactions and communication with the internal tissues and organs require biocompatible and benign interfacing. Various hydrogel interfaces have been incorporated in a wide range of ingestible and minimally invasive devices to offer more favourable tissue–device interactions and communication (FIG. 1c).

Taking advantage of the soft, biocompatible and highly swellable characteristics of hydrogels, several hydrogel-based gastrointestinal-retentive ingestible devices have been developed for health monitoring<sup>58,149</sup>, drug delivery<sup>57</sup> and weight control<sup>150</sup>, including several clinically approved products such as weight control devices based on cellulose hydrogels (TABLE 2). Swollen hydrogels have similar mechanical properties to food, providing favourable mechanical interactions with the gastrointestinal organs during their administration, retention and digestive passage from the body.

Endoluminal insertion and navigation of catheters, guidewires and stents are a routine part of minimally invasive surgeries and daily patient care. However, mechanical interactions of the inserted devices with narrow tubular organs can cause complications such as frictional tissue damage and infection. To alleviate these issues, various hydrogels have been introduced in clinically approved catheters (in particular, polyvinylpyrrolidone hydrogels),

guidewires (in particular, poly(methyl vinyl ether/maleic anhydride) hydrogels) and stents (in particular, poly(methyl vinyl ether/maleic anhydride) hydrogels) in the form of thin coatings to provide soft, low-friction and antifouling interfacing with the endoluminal surface of tubular organs<sup>64,151–156</sup> (TABLE 2).

### Functional modes of hydrogel interfaces

Machines and the human body can interact and communicate via diverse functional modes depending on the desired applications and the characteristics of the target tissues and organs. Hence, hydrogel interfaces bridging machines and the human body also need to incorporate a wide range of functional modes. We classify the functional modes of hydrogel interfaces into six categories: mechanical, acoustic, electrical, optical, chemical and biological (TABLE 3 and FIG. 2).

In addition, because a machine can interface with the human body via multiple functional modes simultaneously, hydrogel interfaces often need to be multifunctional (TABLE 1). For example, epidermal electrodes require hydrogel interfaces to function not only in the electrical mode through electrical conduction but also in the mechanical mode exploiting skin-matching mechanical properties and adhesiveness<sup>5,157</sup>. Therefore, the rationally guided design and development of materials for hydrogel interfaces necessitate the systematic consideration of various functional modes and the corresponding desired properties to enable multifunctional applications. In this section, we discuss the six major functional modes of hydrogel interfaces and the desired properties for each functional mode.

**Mechanical mode.** The mechanical mode of hydrogel interfaces is essential because it guarantees their integrity and robustness as well as their stable adhesion and matching rigidity with the target tissues and organs. Hydrogel interfaces in the mechanical mode are required to possess a set of bulk and interfacial properties (FIG. 2a and TABLE 3).

Many machines and devices require prolonged contact with the human body. For example, wearable devices for health monitoring form close contact with the epidermis for days to weeks. Long-term implantable devices can stay within the body contacting internal tissues and organs over months to years. The various tissues and organs in the human body possess substantially different mechanical stiffness. Mechanical interactions between the target tissues or organs and hydrogel interfaces with dissimilar mechanical stiffness can cause impaired functional efficacy, for example, through non-conformal contact, as well as long-term adverse tissue responses such as foreign-body response, tissue damage or scar formation<sup>2,33,88,114</sup>. Therefore, a desired bulk property of a hydrogel interface is a mechanical stiffness, or Young's modulus, matching that of the target tissue or organ.

The human body is a dynamic system mechanically interacting with external environments and within itself. Hence, hydrogel interfaces also face highly dynamic mechanical interactions with the human body. Preventing bulk failures caused by mechanical loads and deformation is a key design criterion to ensure the

Table 3 | Desired properties of hydrogel interfaces for various functional modes

Property	Design criteria	Target tissues	Relevant clinical applications	Examples
<b>Mechanical mode</b>				
Young's modulus	Young's modulus matching that of the target tissue	Skin, muscle, nerve, internal organs	Wound dressings, tissue adhesives, skin or nerve grafts	GelMA hydrogels <sup>189,190</sup> ; alginate hydrogels <sup>191–193</sup> ; chitosan hydrogels <sup>194–196</sup>
		Tendon, ligament	Tendon replacement	Aligned-nanofiber composite hydrogels <sup>197–201</sup>
		Bone	Bone grafts	Hydroxyapatite-mineralized hydrogels <sup>203,204</sup>
Fracture toughness	High fracture toughness	All tissues	Tendon or cartilage replacement	Double-network hydrogels <sup>158,159</sup> ; nanocomposite hydrogels <sup>160,161</sup>
Interfacial toughness	High interfacial toughness	All tissues	Wound dressings, tissue adhesives, wearable/implantable electrodes	Tough adhesive hydrogels <sup>116,117,162–164</sup> ; hydrogel microneedles <sup>165</sup>
Friction coefficient	Low friction coefficient	Cartilage, meniscus	Cartilage replacement	Hydrogels with repulsive dangling chains <sup>61</sup> ; polymer-filled hydrogels <sup>92,213</sup> ; lipid-incorporating hydrogels <sup>65</sup>
<b>Acoustic mode</b>				
Acoustic impedance	Acoustic impedance matching that of the target tissue	Skin	Ultrasound couplants	Hydrogel ultrasonic couplants <sup>93,169,170</sup>
<b>Electrical mode</b>				
Electrical conductivity	High electrical conductivity	Brain, spinal cord, peripheral nerve, heart, muscle	Wearable/implantable electrodes	Conducting polymer hydrogels <sup>77,221,223</sup> ; CNT-composite hydrogels <sup>219</sup> ; graphene-composite hydrogels <sup>220</sup> ; metal nanowire-composite hydrogels <sup>217,218</sup>
Capacitance	High capacitance			
<b>Optical mode</b>				
Transmittance	High transmittance	Eye	Contact lenses	Silicone hydrogel contact lenses <sup>108</sup>
Refractive index	Tunable refractive index	All tissues	Implantable waveguides	Step-index hydrogel fibres <sup>141,142,174</sup>
<b>Chemical mode</b>				
Diffusivity	Tunable diffusivity	All tissues	Drug delivery	Porous hydrogels <sup>234,235</sup>
Biodegradability	Tunable biodegradability	All tissues	Implantable medical devices	Oxidized alginate hydrogels <sup>239,240</sup>
Binding affinity	High binding affinity to target chemical	All tissues	Wearable/implantable sensors	Glucose-sensing hydrogels <sup>178,247</sup>
<b>Biological mode</b>				
Cell adhesiveness	High cell adhesiveness	All tissues	Tissue scaffolds	RGD peptide-modified hydrogels <sup>252,253</sup>
Foreign-body response	Low foreign-body response	All tissues	Implantable medical devices	Zwitterionic hydrogels <sup>66,70,73</sup> ; anti-FBR drug-eluting hydrogels <sup>258</sup>

CNT, carbon nanotube; FBR, foreign-body response; GelMA, gelatin methacrylate; RGD, arginyl-glycyl-aspartic acid.

**Fracture toughness**

$\Gamma = G_{c,bulk} = -dU_{bulk}/dA$ , where  $G_{c,bulk}$  is the critical energy release rate that drives bulk crack propagation in the material,  $U_{bulk}$  is the total potential energy of the material and  $A$  is the crack area measured in the undeformed state<sup>33,159</sup>. Unit: Jm<sup>2</sup>.

**Interfacial toughness**

$\Gamma^{inter} = G_{c,inter} = -dU_{inter}/dA$ , where  $G_{c,inter}$  is the critical energy release rate that drives interfacial crack propagation,  $U_{inter}$  is the total potential energy of the adhered materials and  $A$  is the crack area measured in the undeformed state<sup>33,162</sup>. Unit: Jm<sup>2</sup>.

reliable functionality of hydrogel interfaces. Thus, a high fracture toughness is another desirable bulk property for hydrogel interfaces<sup>158–161</sup>.

Various applications of hydrogel interfaces, such as epidermal electrodes, tissue adhesives and sealants, require interfacial integration with the target tissues to provide the desired functionality (TABLE 1). Interfacial integration of hydrogel interfaces with the human body requires establishing and maintaining robust adhesion to biological tissues. Adhered hydrogel interfaces can undergo interfacial failures, which can result in functional loss, for example, through the detachment of devices, or detrimental clinical complications such as leakage from failed tissue sealants. To achieve robust interfacial integration, hydrogel interfaces require high interfacial toughness<sup>116,117,162–165</sup>.

Another important function of hydrogel interfaces in the mechanical mode is the reduction of friction and wear with the target tissues and organs. Interfacial

mechanical interactions between hydrogel interfaces and the target tissues and organs can cause frictional wear. Sustained frictional wear can cause the interfacial erosion of poorly lubricated hydrogel interfaces and/or tissue damage. Hence, a low friction coefficient is desirable to minimize frictional wear in applications such as minimally invasive medical devices<sup>64,154</sup> and artificial cartilage<sup>65,166</sup>.

**Acoustic mode.** Owing to its non-destructive and non-invasive nature, the sound wave-based diagnosis of diseases and health conditions has become standard clinical practice<sup>94</sup>. Furthermore, the capability of ultrasound to deliver energy into deep tissues in a non-destructive manner has been utilized in various therapeutic applications, including thermal treatments and non-thermal therapies exploiting mechanical effects, such as ultrasonic lithotripsy<sup>96</sup>, as well as in drug delivery<sup>167,168</sup>. Hence, the acoustic mode of hydrogel interfaces can be

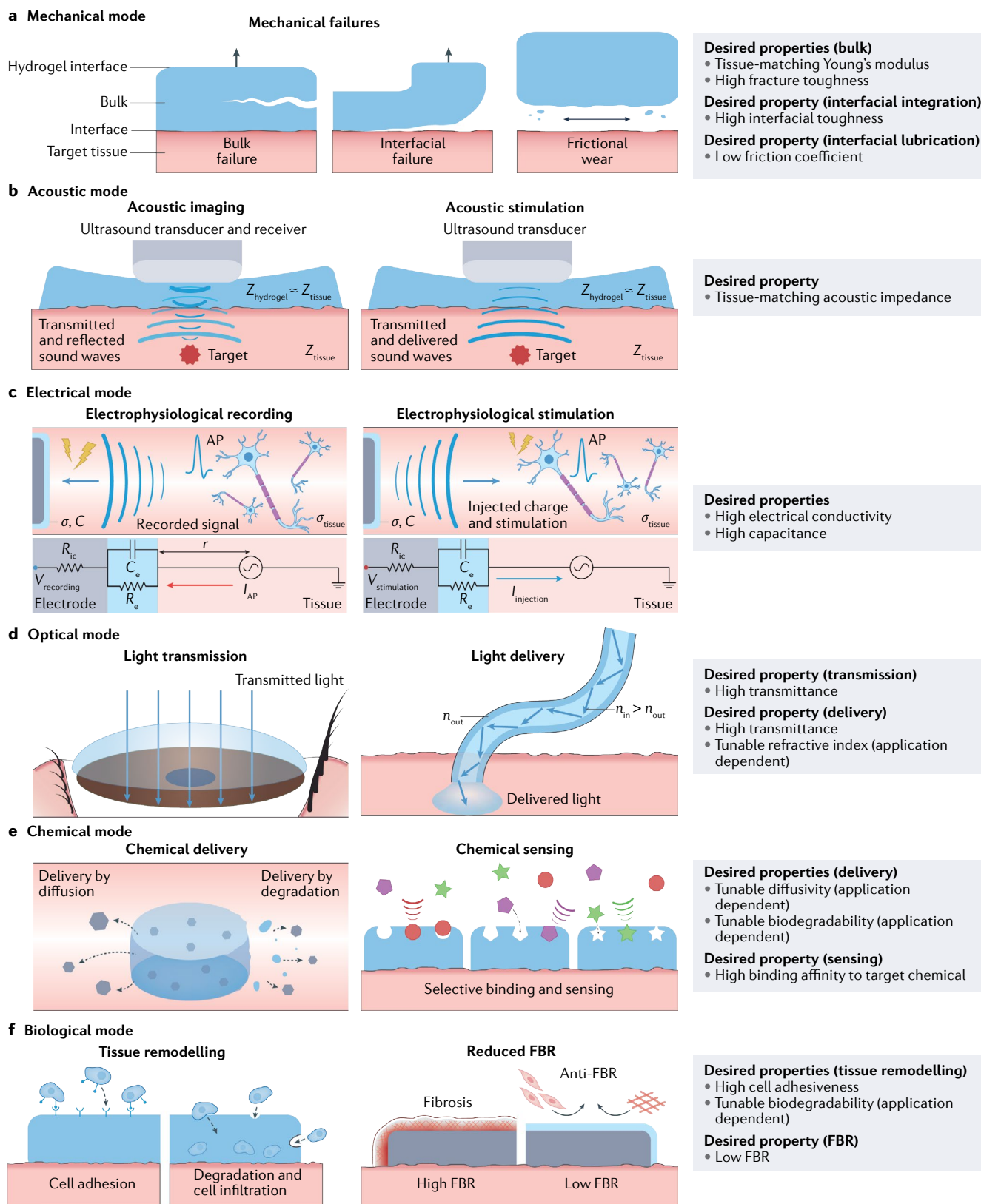


Fig. 2 | **Functional modes of hydrogel interfaces.** Various functional modes of communication and interactions between humans and machines via hydrogel interfaces, including mechanical (part a), acoustic (part b), electrical (part c), optical (part d), chemical (part e) and biological (part f) modes and the desired properties of hydrogel interfaces for each mode.  $\sigma_{tissue}$ , conductivity of the tissue media; AP, action potential;  $C_e$ , capacitance of the hydrogel

interface; FBR, foreign-body response;  $I_{AP}$ , target cell's transmembrane current amplitude of action potential;  $I_{injection}$ , current injected to the target tissue by electrophysiological stimulation;  $r$ , distance between the electrode and the target cell;  $R_e$ , resistance of the hydrogel interface;  $R_{ic}$ , interconnect resistance;  $V_{recording}$ , electric potential of the electrophysiological recording;  $V_{stimulation}$ , applied electric potential for electrophysiological stimulation.



**Friction coefficient**

$\mu = f/N$ , where  $f$  is the measured friction force and  $N$  is the applied normal force to the material. Unitless.

**Acoustic impedance**

For a homogeneous material, the acoustic impedance is  $Z = \sqrt{\rho_{\text{eff}} K_{\text{eff}}}$ , where  $\rho_{\text{eff}}$  is the effective density and  $K_{\text{eff}}$  is the effective bulk modulus of the material. Unit:  $\text{Pa}\cdot\text{sm}^{-3}$ .

**Transmittance**

$T = I/I_0$ , where  $I_0$  is the intensity of incident light and  $I$  is the intensity of transmitted light through the material. Unitless and often denoted in percentage.

exploited for two types of applications: acoustic imaging by facilitating the delivery of sound waves to and reflection from the target, such as in ultrasonography, and acoustic stimulation by facilitating the delivery of sound waves to the target such as in ultrasonic lithotripsy (FIG. 2b).

Ultrasonic transducers and probes used for these applications are made of conventional materials with an acoustic impedance substantially different from that of skin<sup>33</sup>. Furthermore, the high mechanical rigidity of the ultrasonic transducers and probes prevents their conformal interfacial contact with skin, resulting in air-filled gaps that also have disparate acoustic impedance compared to skin. The resultant mismatch in acoustic impedance at the skin–probe interface can severely hinder the transmission of acoustic waves owing to interfacial reflections and scattering<sup>169</sup>, deteriorating functional efficacy (for example, decreasing the quality of sonographic images). Hence, tissue-matching acoustic impedance and conformal interfacial contact with skin are advantageous for hydrogel interfaces that work in the acoustic mode<sup>93,169,170</sup> (FIG. 2b and TABLE 3).

**Electrical mode.** Machines can communicate and interact with electrically active tissues and organs in the human body, such as the brain, nerves, muscles and heart, through hydrogel interfaces functioning in the electrical mode<sup>5</sup>. The electrical mode of hydrogel interfaces can be used in two types of applications based on the direction of electrical communication: from the human body to hydrogel interfaces for electrophysiological recording, and from hydrogel interfaces to the human body for electrophysiological stimulation (FIG. 2c and TABLE 3).

Based on a simplified equivalent circuit model<sup>5</sup> (FIG. 2c), the electrical potential in electrophysiological recording and the injected current in electrophysiological stimulation can be quantitatively expressed as:

$$V_{\text{recording}} = \frac{1}{4\pi\sigma_{\text{tissue}}r} \left[ \left( \frac{1}{R_e} + sC_e \right) R_{ic} \right] I_{\text{AP}} \quad (1)$$

$$I_{\text{injection}} = \left[ \left( \frac{1}{R_e} + sC_e \right)^{-1} + R_{ic} \right]^{-1} V_{\text{stimulation}} \quad (2)$$

where  $\sigma_{\text{tissue}}$  is the conductivity of the tissue,  $r$  is the distance between the electrode and the target cell,  $R_e$  is the resistance of the hydrogel interface,  $s$  is the complex frequency of the action potential (for recording) or the stimulation waveforms (for stimulation),  $C_e$  is the capacitance of the hydrogel interface,  $R_{ic}$  is the interconnect resistance,  $I_{\text{AP}}$  is the target cell's transmembrane current amplitude of action potential,  $I_{\text{injection}}$  is the current injected to the target tissue by the electrophysiological stimulation, and  $V_{\text{stimulation}}$  is the applied electric potential for electrophysiological stimulation<sup>5</sup>.

In electrophysiological recording, a high  $V_{\text{recording}}$  is desirable. Hence, for given physiological ( $\sigma_{\text{tissue}}$ ,  $r$ ,  $s$ ,  $I_{\text{AP}}$ ) and recording ( $R_{ic}$ ) conditions, high electrical

conductivity (low  $R_e$ ) and high capacitance (high  $C_e$ ) are advantageous. Notably, physiological environments exhibit native ionic conductivity ( $0.3\text{--}0.7 \text{ Sm}^{-1}$ )<sup>19,171</sup> because of the high water content of biological tissues (BOX 1) and their rich ionic compositions comprised of salts and charged proteins. Hence, the electrical conductivity of hydrogel interfaces should be substantially higher than that of the surrounding tissue to ensure the quality of recorded signals<sup>5,172,173</sup>.

In electrophysiological stimulation, a high  $I_{\text{injection}}$ , often measured as charge injection capacity, is desirable. Hence, for a given stimulation device ( $R_{ic}$ ) and input ( $V_{\text{stimulation}}$ ), high electrical conductivity (low  $R_e$ ) and high capacitance (high  $C_e$ ) are advantageous. Therefore, high electrical conductivity and high capacitance are desirable properties of hydrogel interfaces in the electrical mode for both recording and stimulation applications.

**Optical mode.** The optical mode of hydrogel interfaces relies on the transmission and delivery of light to the human body (FIG. 2d and TABLE 3). Unblocked transmission of incident light to the eye is a critical requirement for visual functionality and eyesight. Hence, hydrogel interfaces for ophthalmic applications require high transmittance to minimize the attenuation of transmitted light to the eye<sup>108,110</sup>. Beyond ophthalmic interfacing, the delivery of a broad spectrum of light to diverse tissues and organs is enabling the use of hydrogel interfaces for photonic diagnosis and treatment<sup>110</sup>. Light delivery requires an optical pathway typically in the form of a waveguide that provides directional guidance for the transmitted light, where the transmittance and refractive index respectively modulate the transmission and internal reflection of light<sup>143,144</sup>. Therefore, hydrogel interfaces for light delivery require high transmittance and a tunable refractive index<sup>141,142,174</sup>.

**Chemical mode.** Physiological activities involve diverse chemical processes and reactions and, therefore, chemical interactions with the human body are one of the key functional modes of hydrogel interfaces. The high water content of biological tissues and hydrogel interfaces inherently allows the exchange of waterborne chemicals. Based on the direction of the chemical communication, the chemical mode of hydrogel interfaces can be further divided into two types: from hydrogel interfaces to the human body for chemical delivery, and from the human body to hydrogel interfaces for chemical sensing (FIG. 2e and TABLE 3).

Chemical delivery is commonly utilized for the administration of pharmacological substances, such as drugs and other biologics, for therapeutic interventions and treatments<sup>84,86,87,145</sup>. The therapeutic efficacy and toxicity of drugs are highly sensitive to their dosage and release profile; therefore, the capability to engineer controlled release from hydrogel interfaces is a critical requirement<sup>145</sup>. Chemicals within hydrogel interfaces can be released to the surrounding tissue by diffusion or by degrading the hydrogel. The rate and profile of chemical delivery by diffusion are determined by the specific diffusivity of the chemicals in the hydrogel<sup>84</sup>, whereas the rate and profile of chemical delivery by

hydrogel degradation rely on the biodegradability of the hydrogel<sup>84</sup>. Because different drugs have different sizes and interactions with hydrogel matrices, tunable mesh sizes, interactions with chemicals (such as binding and release) and/or biodegradability are highly desirable for chemical delivery<sup>87</sup>.

The sensing of a certain chemical species requires selectivity in interactions between the target chemical and hydrogel interfaces<sup>146,175–179</sup>. This selectivity can be controlled by tuning the binding affinity to the target chemical as a higher binding affinity provides a higher selectivity<sup>177</sup>. Hence, a high binding affinity to target chemicals is desirable for selective chemical sensing.

**Biological mode.** Interfaces between machines and biological tissues inherently involve a broad range of biological interactions that substantially influence the machines' efficacy, reliability and biosafety. As a result, the biological mode of hydrogel interfaces is of essential importance, especially in applications that require higher invasiveness and long-term interactions with the human body such as implantable devices. The biological mode of hydrogel interfaces can be divided into various types depending on the application requirements: promotion of biological activities (such as cell adhesion, proliferation, infiltration and differentiation) and suppression of biological activities (such as anti-foreign-body responses)<sup>180</sup> (FIG. 2f and TABLE 3).

Cell adhesion and infiltration to hydrogel interfaces and subsequent partial or full remodelling of the hydrogel interfaces by native tissues are favourable for various implantable applications. For example, implanted devices for drug delivery and tissue repair (such as tissue adhesives and sealants) require the gradual infiltration of cells from the surrounding tissue with ultimate resorption and tissue remodelling to avoid the need for surgical removal of the devices and potential long-term adverse effects such as chronic inflammation<sup>87,114,181</sup>. Cellular interactions and tissue remodelling processes rely on the initial attachment of cells to the hydrogel, which is followed by the progressive degradation of the hydrogel and infiltration of cells<sup>31,35,81,182,183</sup>. Hence, high cell adhesiveness and biodegradability are important in applications where tissue remodelling is desired.

Regulating unfavourable biological interactions between the implanted device and the surrounding tissue is also an important function of hydrogel interfaces. Biofouling and foreign-body response in physiological environments and the resultant fibrosis can be detrimental to the long-term efficacy of hydrogel interfaces<sup>4,23</sup>. Because fibrotic encapsulation and scar tissues possess much lower electrical conductivity and chemical diffusivity than native tissues, they substantially reduce the efficacy of electrical sensing and stimulation<sup>2–5,173,184</sup> as well as of chemical delivery and sensing<sup>9,23,185–188</sup>. Therefore, a low foreign-body response is highly desirable for efficient long-term communication in the electrical, chemical and optical modes<sup>28,185,188</sup>.

**Hydrogel–machine interfaces.** In addition to hydrogel–tissue interfaces, interfaces between hydrogels and machines are also important. To avoid interfacial failure

between hydrogels and machines, hydrogel–machine interfaces require robust integration with high interfacial toughness<sup>162,163</sup>. For the acoustic, electrical and optical modes of hydrogel interfaces, the robust integration between hydrogels and machines should also provide high acoustic transmittance, high optical transparency<sup>162</sup> and high electrical conductivity<sup>139</sup>, respectively. In addition, chemical delivery and sensing can be performed by a machine, such as a drug reservoir or a sensor coated in the hydrogel, instead of by the hydrogel itself. In this case, a high permeability or diffusivity of the chemicals at the hydrogel–machine interface is required to allow unhindered transportation of chemicals between the target tissue and the machine<sup>87</sup>. This Review focuses primarily on hydrogel–tissue interfaces but several reviews are available that discuss hydrogel–machine interfaces<sup>33,34,88</sup>.

### Design principles for hydrogel interfaces

Enabling the functional modes of hydrogel interfaces requires the implementation of various desired hydrogel properties (TABLE 3). Although hydrogels can offer diverse properties, achieving optimal properties for a desired functional mode is complex<sup>33,37</sup>. As a result, Edisonian approaches based on trial and error have limited success<sup>5,33</sup>, particularly for the development of multifunctional hydrogel interfaces.

In this section, we summarize rational design principles to achieve desired properties for hydrogel interfaces, providing some examples from the literature (TABLE 3 and FIG. 3).

**Mechanical properties.** Mechanical interactions between hydrogel interfaces and the human body are affected by the hydrogel bulk and interfacial mechanical properties, including Young's modulus, fracture toughness, interfacial toughness and friction coefficient (FIG. 2a). Because the mechanical properties of tissues are determined by their compositional and structural features, the design principles for the mechanical properties of hydrogel interfaces are largely based on mimicking the target tissue compositional and/or structural characteristics.

Soft tissues (which include skin, muscle, nerve and internal organs) have relatively low Young's moduli (1 kPa to 10 MPa) owing to their crosslinked extracellular matrices (BOX 1). Conventional hydrogels consisting of crosslinked polymer networks show compositional and structural similarities with soft tissues, including low Young's moduli<sup>33</sup>. The Young's moduli of conventional hydrogels can be tuned by controlling the density of polymer chains per unit volume,  $n$ , as follows:

$$E_{\text{hydrogel}} \sim nkT \quad (3)$$

where  $k$  is the Boltzmann constant and  $T$  is the absolute temperature<sup>33</sup>;  $n$  can be engineered by varying the polymer concentration and the crosslink density of the hydrogel<sup>33</sup>. Hence, diverse conventional hydrogels with varying compositions (for example, GelMA hydrogels<sup>189,190</sup>, alginate hydrogels<sup>191–193</sup> or chitosan hydrogels<sup>194–196</sup>) have been adopted in hydrogel interfaces to provide tissue-matching Young's moduli.

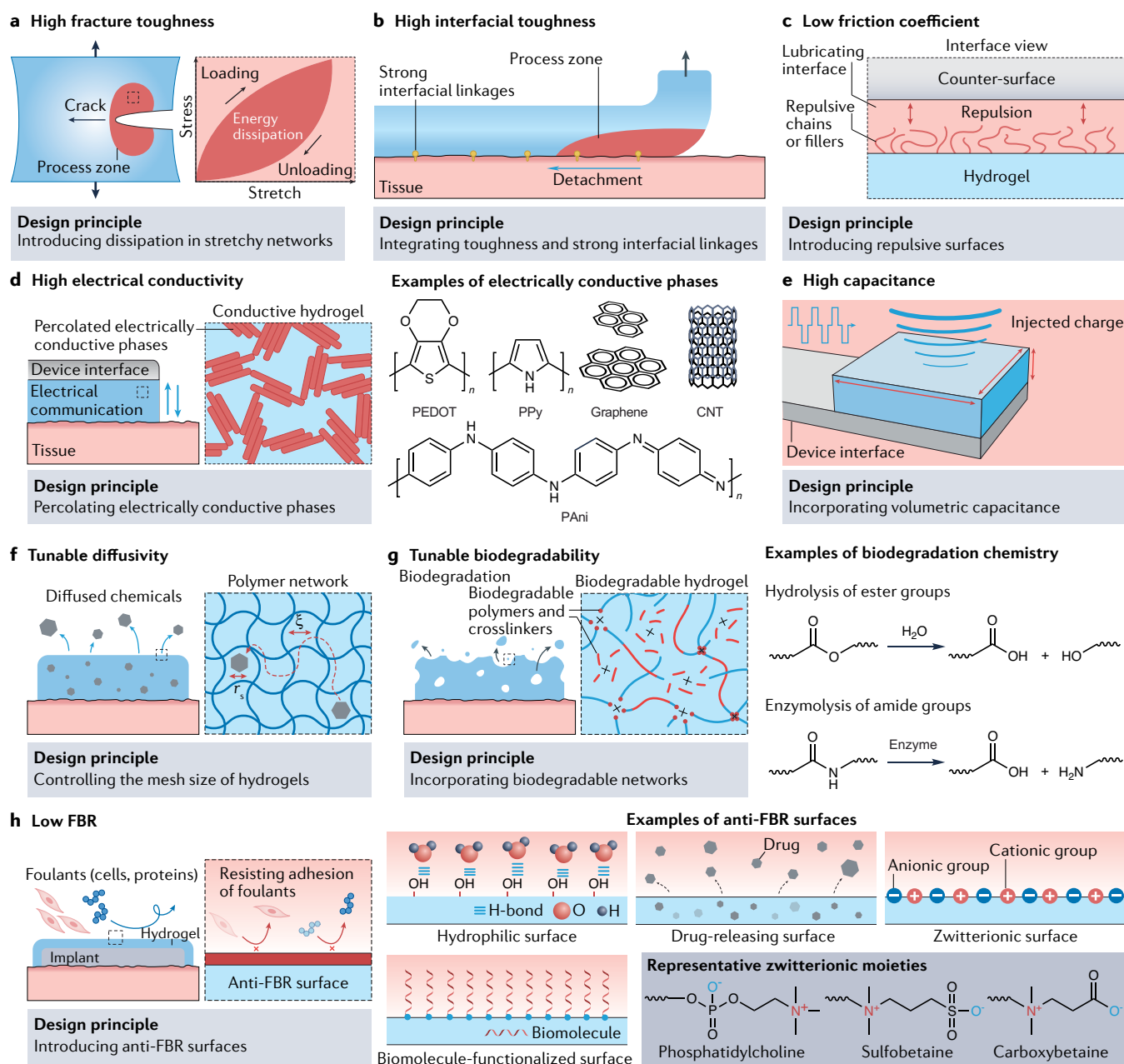


**Fig. 3 | Design principles for hydrogel interfaces with desired properties.** Rational design principles to achieve desired properties for hydrogel interfaces, including mechanical properties such as high fracture toughness<sup>36,158,159</sup> (part a), high interfacial toughness<sup>162,163,209</sup> (part b) and low friction coefficient<sup>212</sup> (part c); electrical properties such as high electrical conductivity<sup>5,217–219,223</sup> (part d) and high capacitance<sup>5,77,221</sup> (part e); chemical properties such as tunable diffusivity<sup>230–232</sup> (part f) and tunable biodegradability<sup>181,269</sup> (part g); and biological properties such as a low foreign-body response (FBR)<sup>28,70,73,75,188,258</sup> (part h). The grey dotted boxes provide an enlarged view of selected areas.  $\xi$ , mesh size of the hydrogel polymer network; CNT, carbon nanotube; H-bond, hydrogen bond; PANi, polyaniline; PEDOT, poly(3,4-ethylenedioxythiophene); PPy, polypyrrole;  $r_s$ , radius of the chemical.

Stiff connective tissues, such as tendons and ligaments, exhibit significantly higher (10 MPa to 1 GPa) and anisotropic (stiffer in the longitudinal direction) Young's moduli than soft tissues. These properties largely originate from their highly aligned fibrous microstructures<sup>197</sup>. Several strategies using synthetic polymers such as polyvinyl alcohol and biopolymers such as alginate, silk and cellulose<sup>197–201</sup> have achieved aligned fibrous hydrogels that are tendon-like. Bone tissues show very high

Young's moduli (1–30 GPa) owing to the rich mineral contents of their main component, hydroxyapatite<sup>202</sup>. Hence, several bone-matching hydrogel interfaces have been developed by incorporating a high concentration of hydroxyapatite within the hydrogel matrix<sup>203,204</sup>.

Notably, additional considerations can arise for specific applications. For instance, hydrogel interfaces with a Young's modulus higher or lower than that of the target tissue can influence cellular responses via

mechanotransduction, a mechanism that modulates various biological processes<sup>205</sup> such as cell migration (for example, fibroblast migration towards a substrate with higher Young's modulus), proliferation or differentiation (for example, promoted osteoblast differentiation on a substrate with higher Young's modulus). Moreover, beyond Young's modulus, rate-dependent mechanical properties, such as viscoelasticity and poroelasticity, can be beneficial for certain applications, including tissue engineering<sup>83,206</sup> and bioelectronics<sup>78,207</sup>, to match the mechanical properties of the target tissue.

To achieve high fracture toughness, mechanical dissipation and stretchability must be synergistically combined<sup>33,36,208</sup> (FIG. 3a). The resultant fracture toughness can be expressed as follows:

$$\Gamma = \Gamma_0 + \Gamma_D \quad (4)$$

where  $\Gamma_0$  is the intrinsic fracture toughness and  $\Gamma_D$  is the contribution of the mechanical dissipation in the process zone (the region ahead of the crack tip that dissipates mechanical energy) to the total fracture toughness<sup>36,159</sup>. Because the intrinsic fracture toughness of conventional hydrogels is commonly limited to 10–100 Jm<sup>-2</sup>, high mechanical dissipation is needed for high fracture toughness<sup>36</sup>. The mechanical dissipation of a hydrogel within the process zone is proportional to the area of the hysteresis loop in its stress–stretch curve during a loading–unloading cycle (FIG. 3a). Various strategies to provide high mechanical dissipation have been developed, such as using double-network hydrogels<sup>158,159</sup> (hydrogels consisting of two interpenetrating networks) and nanocomposite hydrogels<sup>160,161</sup> (hydrogels containing nanoscale crosslinkers), to introduce sacrificial networks and bonds into hydrogels.

To achieve high interfacial toughness for hydrogels adhered to tissues, high fracture toughness and strong interfacial linkages between the hydrogel and tissue need to be synergistically integrated<sup>33,162</sup> (FIG. 3b). The resultant interfacial toughness can be expressed as follows:

$$\Gamma^{\text{inter}} = \Gamma_0^{\text{inter}} + \Gamma_D^{\text{inter}} \quad (5)$$

where  $\Gamma_0^{\text{inter}}$  is the intrinsic interfacial toughness from the interfacial linkages and  $\Gamma_D^{\text{inter}}$  is the contribution of the mechanical dissipation in the process zone<sup>162,209</sup>. High intrinsic interfacial toughness can be achieved by strong interfacial linkages between the hydrogel and the tissue. Mechanisms that provide strong interfacial linkages between tough dissipative hydrogels and biological tissues or machines include covalent bonds<sup>19,117,210</sup> (such as amide bonds), high-density hydrogen bonds<sup>211</sup> (such as in dry-annealed polyvinyl alcohol hydrogels) and topological interpenetration of polymers<sup>116,164</sup> (such as in topologically interpenetrating chitosan solutions).

By making the hydrogel surface non-adhesive, low friction coefficients between hydrogels and tissue surfaces can be achieved<sup>63,212</sup> (FIG. 3c). Non-adhesive hydrogel surfaces with low friction coefficients have been developed based on the incorporation of various lubricating components, including non-adhesive dangling chains<sup>61</sup> (such as for poly(2-acrylamido-2-methyl-1-propanesulfonic

acid) hydrogels synthesized on Teflon substrates), uncrosslinked polymers<sup>62,213</sup> (such as for porous polyacrylamide hydrogels filled with uncrosslinked alginate) and lipids<sup>65</sup> (such as for poly(hydroxyethylmethacrylate) hydrogels with incorporated phosphatidylcholine lipids). In these hydrogels, the lubricating components provide non-adhesive surfaces against the counter surfaces, resulting in highly lubricated interfaces with low friction coefficients.

**Acoustic properties.** Tissue-matching acoustic impedance is critical to minimize interfacial reflection or scattering of acoustic waves in the acoustic mode<sup>214</sup>. The acoustic impedance of a homogenous material is determined by the effective density and bulk modulus of the material. Hence, to match the acoustic impedance of biological tissues, the effective density and bulk modulus of the hydrogel interfaces must correspond to those of the target tissue<sup>94</sup>. Notably, because the effective density and bulk modulus of hydrogels with high water content are almost the same as those of water<sup>215</sup>, the acoustic impedance is approximately the same as that of water-rich biological tissues<sup>93,169,170</sup>. For example, hydrogels with a high water content based on polyacrylamide, polyvinyl alcohol, polyacrylic acid and poly(hydroxyethylmethacrylate) have been adopted as acoustic couplants in both academic and clinical settings<sup>93,95,216</sup> (TABLE 2).

**Electrical properties.** Electrical conductivity is commonly introduced to hydrogels by incorporating electrically conductive phases<sup>5</sup>. However, if these phases are non-continuous, they cannot effectively transport electrical currents. Hence, the percolation of electrically conductive phases within hydrogel interfaces is needed for high electrical conductivity (FIG. 3c). Various conductive fillers, including metal nanowires<sup>217,218</sup> (such as Ag and Au), carbon nanotubes<sup>219</sup>, graphene<sup>19,220</sup> and conducting polymers<sup>137</sup> (such as poly(3,4-ethylenedioxythiophene):poly(styrene sulfonate), polypyrrole and polyaniline), have been used to form percolated electrically conductive phases in hydrogel interfaces (FIG. 3d). Notably, hydrogel interfaces purely consisting of percolated conducting polymers have been developed and show very high electrical conductivity<sup>77,138,221–223</sup>.

The capacitance of metallic electrodes is typically low because it originates from the surface-bound electrical double layer<sup>5</sup>. Low capacitance at the electrode–tissue interface can result in high electrical impedance and inefficient charge injection, which are highly undesirable for electrophysiological recording and stimulation, respectively<sup>5,172</sup>. Incorporating volumetric capacitance into the hydrogels to overcome the limitation of the surface-bound electrical double layer can help in achieving high capacitance<sup>5</sup> (FIG. 3e). To incorporate volumetric capacitance, conducting polymer-based hydrogel interfaces have been developed that can form electrical double layers in the nanoporous structure of the conducting polymers<sup>224,225</sup>. For example, conducting polymer hydrogels based on poly(3,4-ethylenedioxythiophene):poly(styrene sulfonate) have high volumetric capacitance, low impedance and high charge injection capacity in wet

**Electrical double layer**

Accumulation of charged ions around the electrode within electrolytic medium under the applied electric potential.



physiological environments, which are required for in vivo electrophysiological modulation<sup>77,138,139,223</sup>.

**Optical properties.** The transmittance of light in materials is determined by the degree of scattering and blockage of the incident light within the material. When the size of the hydrogel constituents (for example, the polymer aggregates or crystalline domains) is greater than one-tenth of the wavelength of the incident light, light scattering becomes substantially higher, resulting in decreased transmittance<sup>226</sup>. Hence, to achieve high transmittance, light scattering must be minimized by limiting the size of the hydrogel constituents. This design principle has been implemented by minimizing the size of phase-separated polymer-rich and water-rich domains<sup>141</sup> (such as for polyethylene glycol hydrogels with high molecular weight) and by fabricating nanoscale semi-crystalline domains<sup>227</sup> (such as for nanocellulose-reinforced polyvinyl alcohol hydrogels) to achieve hydrogel interfaces with high optical transparency.

Light delivery through optical waveguides relies on total internal reflection, which requires a higher refractive index for the internal medium than for the external medium<sup>141</sup>. Hence, it is critical to ensure that the refractive index of the hydrogel is higher than that of the target tissue<sup>141</sup> or the cladding material<sup>141,142,174</sup>. The refractive indices of hydrogels are inversely proportional to the hydrogel water content, ranging between the refractive index of pure water ( $n = 1.331$ ) and that of pure polymers ( $n = 1.4 - 1.7$ )<sup>141</sup>. Hence, the refractive index can be tuned by controlling the water content of the hydrogel interfaces. For example, step-index hydrogel optical fibres have been developed based on a hydrogel core (such as with polyethylene glycol hydrogels) and cladding (such as with alginate hydrogels) with a varying equilibrium water content<sup>142,174</sup>.

**Chemical properties.** The diffusivity of chemicals in hydrogel interfaces ( $D_{\text{hydrogel}}$ ) is determined by the interactions between the chemicals and the polymer networks of the hydrogel<sup>228,229</sup>. In particular, the relative size of the chemicals (their radius  $r_s$ ) and of the hydrogel network (the mesh size  $\xi$ ) significantly affect chemical diffusivity<sup>87,145</sup>:

$$\frac{D_{\text{hydrogel}}}{D_{\text{water}}} \sim \exp\left(-\frac{r_s}{\xi}\right) \quad (6)$$

where  $D_{\text{water}}$  is the diffusivity of the chemical in water<sup>230-232</sup>.

When the size of the chemical is smaller than the hydrogel mesh size, the chemical can diffuse freely within the hydrogel. Otherwise, the diffusion of the chemical is substantially slowed by steric hindrances from the polymer network. Hence, choosing the mesh size based on the size of the chemical employed for delivery or sensing tunes the diffusivity of the chemical in hydrogel interfaces (FIG. 3f). The mesh size of hydrogels depends on various parameters such as water content and crosslinking density<sup>31-33,87</sup>. To further increase the diffusivity of chemicals, hydrogel interfaces with nanostructures<sup>233</sup> (such as poly(amidoamine) dendrimers), microscopic

or macroscopic porosity<sup>234,235</sup> (such as porous alginate hydrogels), and stimuli responsiveness<sup>236</sup> (such as poly(*N*-isopropylacrylamide)) have also been developed. Several reviews discuss diffusivity in hydrogel interfaces<sup>86,87,237,238</sup>.

The degradation of hydrogels mostly relies on breaking the network building blocks (for example, polymer chains or crosslinks) and thus losing mass to the surrounding physiological environment. Hence, the biodegradability of hydrogel interfaces depends on the incorporation of biodegradable building blocks<sup>181</sup> (FIG. 3g, left). The rate of biodegradation can be controlled by engineering the ratio of degradable building blocks to their non-degradable counterparts. The biodegradation of hydrogel interfaces depends on two major mechanisms: hydrolysis and enzymolysis (FIG. 3g, right). In wet physiological environments, water drives the hydrolysis of ester groups. For example, introducing ester groups in the networks produces hydrolytically biodegradable hydrogel interfaces, such as oxidized alginate<sup>239,240</sup> and polyethylene glycol<sup>241,242</sup>. Hydrogel interfaces containing biopolymers can undergo biodegradation via enzymolysis. Cells and physiological fluids in the human body are rich in enzymes that can cleave and digest various chemical bonds (for example, amide groups) in biopolymers such as collagen<sup>31</sup>, gelatin<sup>189,190</sup>, hyaluronic acid<sup>243</sup> and chitosan<sup>194-196</sup>.

To achieve a high binding affinity to target chemicals, binding components such as ligands have to be incorporated into the hydrogel interfaces<sup>146,175,177,244</sup>. Hydrogel interfaces developed for the sensing of diverse chemicals (for example, glucose or reactive oxygen species) or chemical groups in cells (for example, B cells) incorporate the corresponding ligands or active functional groups<sup>178,245-248</sup> (such as glucose oxidase for glucose and T cells for B cells) into the network. Notably, the high binding affinity between drugs and ligands in hydrogel interfaces can also be used for the controlled release of drugs in the human body<sup>175</sup> (for example, polyacrylamide hydrogels coupled with the GyrB protein used for the triggered release of vascular endothelial growth factor)<sup>21</sup>. Several other reviews address the design of hydrogel interfaces for chemical sensing and release<sup>176,177,246</sup>.

**Biological properties.** Cells adhere to substrates through the binding of proteins such as of integrins to ligands on the surface<sup>249</sup>. Hence, incorporating cell-adhesive ligands into hydrogel interfaces provides cell adhesiveness. Because various biopolymers in the extracellular matrix (such as collagen, gelatin or hyaluronic acid) possess integrin-binding ligands, cells can readily adhere to hydrogel interfaces containing these biopolymers<sup>31</sup>. Specific cell-adhesive proteins (such as fibronectin)<sup>250,251</sup> and peptide motifs (such as arginyl-glycyl-aspartic acid (RGD))<sup>252,253</sup> have also been incorporated for cell adhesiveness.

To achieve a low foreign-body response, hydrophilic, biomolecule-functionalized, zwitterionic and drug-releasing surfaces have been introduced to hydrogels<sup>28,67,188</sup> (FIG. 3h). Hydrophilic surfaces form a hydration layer as a result of bonding with water



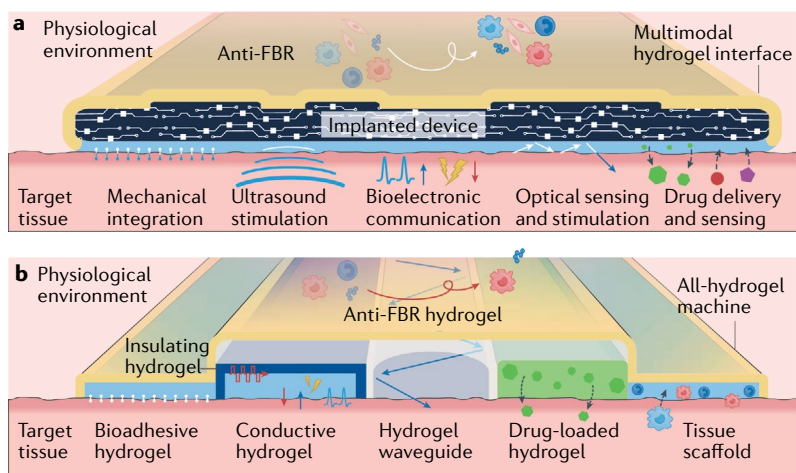


**Fig. 4 | Next-generation hydrogel interfaces. a** | A multimodal hydrogel interface providing multifunctional interfacing between a machine (implanted device) and a target tissue. **b** | An all-hydrogel machine providing a multifunctional interface to a target tissue. FBR, foreign-body response.

molecules in wet physiological environments<sup>254</sup>. The hydration layer acts as a physical barrier against the adhesion of foulants (such as proteins and cells)<sup>255</sup>. Physical barriers against foulants, based on various surface-functionalized biomolecules such as antimicrobial peptides<sup>256,257</sup>, have also been introduced to hydrogels. Furthermore, zwitterionic polymers have also been widely utilized to form anti-foreign-body response surfaces<sup>75</sup>. Poly(phosphatidylcholine), poly(sulfobetaine) and poly(carboxybetaine) are the most commonly adopted zwitterionic polymers that can form hydrogels or that can be grafted to other hydrogel networks<sup>66,70,73</sup>. Apart from various physical barriers, drug-releasing surfaces have been explored to gradually elute anti-foreign-body response drugs from the surfaces of hydrogels<sup>258</sup>.

Notably, various biologically important functional groups can be introduced to hydrogel interfaces to facilitate desirable cell or tissue responses (for example, cell proliferation or differentiation) beyond cell adhesion and anti-foreign-body response. Several reviews offer more detailed discussions<sup>31,81,183,259</sup>.

### Future perspectives

Recent advances in diverse applications have shown the great promise of hydrogel interfaces for the bridging of the human body and machines (FIG. 1); however, there are remaining challenges and opportunities for future developments to effectively achieve this. The importance of continued innovations is particularly highlighted by the stark limitations in establishing long-term functional interfaces between implantable devices and the human body. Despite tremendous progress in implantable devices and hydrogel interfaces for therapeutic, diagnostic and assistive applications in recent decades, the loss of function and failure of long-term implants in the human body owing to suboptimal integration with the target tissues, tissue damage, foreign-body response and/or fibrotic isolation of the implants remain unsolved problems<sup>4,188</sup>. Hence, the development of next-generation

hydrogel interfaces should focus on addressing these challenges using multidisciplinary investigations and rationally guided design rules. In this section, we discuss future perspectives based on two conceptual next-generation hydrogel interfaces (FIG. 4a,b).

**Multimodal hydrogel interfaces.** In the human body, internal organs are integrated with one another by connective tissue to form robust, seamless and multifunctional interfaces. The internal organs also maintain anatomical boundaries without adhesion by serous membranes (or serosa) at their outermost surfaces. These characteristics provide inspiration for multimodal hydrogel interfaces for seamlessly integrated, long-term and multifunctional devices.

For epidermal and wearable applications, multimodal hydrogel interfaces can offer multifunctional interfacing between the skin and various sensors and devices. For instance, advanced wound dressings may require hydrogel interfaces with multiple modes of interaction, including mechanical integration to the skin, electrical, optical, acoustic and chemical sensing for wound monitoring, and chemical delivery of therapeutic substances<sup>53</sup>. For ingestible and minimally invasive applications, multimodal hydrogel interfaces can potentially offer new treatment strategies by synergistically combining various functionalities. For example, low-friction, conductive, transparent and drug-releasing hydrogel coatings on catheters, guidewires or stents may provide electrical and/or optical monitoring of the target tissues and delivery of drugs on top of the conventional clinical treatments offered by minimally invasive medical devices<sup>260,261</sup>. For implantable applications, anti-foreign-body response hydrogel interfaces around the implanted device may provide a long-term functional interface to the human body, similar to serosa in organs (FIG. 4a). Similar to connective tissue in organs, bio-integrative hydrogel interfaces between the implanted device and the target tissue may provide seamless and multifunctional interfacial integration with the human body.

To achieve multimodal hydrogel interfaces, new hydrogels with improved properties will be required. To minimize the foreign-body response, hydrogels with improved efficacy and longevity in diverse tissue environments must be developed. Bio-integration also requires tissue adhesive hydrogels capable of long-term integration to the target tissue without inflammatory responses and subsequent fibrotic encapsulation. Furthermore, there is a need to address potential tradeoffs between different properties and functional modes of hydrogel interfaces. For example, increasing the electrical conductivity of a hydrogel interface often leads to less favourable mechanical (such as stretchability, fracture toughness and interfacial toughness) and optical (such as transparency) properties<sup>5</sup>.

**All-hydrogel machines.** Existing devices are mostly composed of conventional materials, such as metals, plastics and elastomers, that are dissimilar to biological tissues. By contrast, biological tissues and organs (except teeth, nails and bones) are essentially multifunctional structures fully consisting of hydrogels seamlessly integrating

cells and extracellular matrices. Hence, biological tissues and organs not only serve as applicational targets but also provide inspiration for all-hydrogel machines (FIG. 4b).

Because of their tissue-like composition and properties, all-hydrogel machines offer promise for the improvement of device biocompatibility. Furthermore, the absence of conventional materials can potentially enable functional devices that are truly transient and tissue-integrative by allowing the ultimate biodegradation and tissue in-growth of the all-hydrogel machine without leaving residual materials. Although all-hydrogel machines may benefit a broad range of applications, they would be particularly advantageous for implantable applications where biocompatibility, degradation and tissue integration are critical requirements<sup>207</sup>.

The realization of all-hydrogel machines will require the development of hydrogels with new and improved properties. For example, conductive hydrogels with improved electrical properties (such as electrical conductivity and capacitance) and hydrogel waveguides with optimized optical properties (such as transmittance and refractive index) must be developed to successfully replace existing metal-based electrodes and stiff optical waveguides, respectively. Similar to multimodal hydrogel interfaces, bio-integration and an improved anti-foreign-body response will be critical to ensuring the long-term functional preservation of all-hydrogel

machines in physiological environments. Hydrogels with new properties, such as electrically semiconducting and insulating properties, will require novel materials to replace existing silicon-based semiconductors and plastic-based or elastomer-based insulators, respectively. Furthermore, synergistically with material developments, new and advanced fabrication strategies should be developed to manufacture future all-hydrogel machines. While various advanced fabrication methods, such as photolithography and additive manufacturing, have been utilized for individual hydrogel materials, manufacturing of all-hydrogel machines consisting of a broad range of hydrogels with diverse functionalities in a highly integrated and precise manner would necessitate further improvement of existing methods and development of new fabrication strategies.

Overall, hydrogel interfaces will play an essential role towards the futuristic vision of a seamless merger of machines and humans. Despite a promising outlook, hydrogel interfaces will undoubtedly face numerous scientific, engineering and translational challenges during future development and implementation. However, in our wildest imagination, hydrogel interfaces may one day allow us to blur the boundary between biological and abiotic systems and may enable future human-machine hybrids.

Published online 13 October 2022

- Jeong, J.-W. et al. Soft materials in neuroengineering for hard problems in neuroscience. *Neuron* **86**, 175–186 (2015).
- Lacour, S. P., Courtine, G. & Guck, J. Materials and technologies for soft implantable neuroprostheses. *Nat. Rev. Mater.* **1**, 16063 (2016).
- Salatino, J. W., Ludwig, K. A., Kozai, T. D. & Purcell, E. K. Glial responses to implanted electrodes in the brain. *Nat. Biomed. Eng.* **1**, 862–877 (2017).
- Lotti, F., Ranieri, F., Vadalà, G., Zollo, L. & Di Pino, G. Invasive intraneural interfaces: foreign body reaction issues. *Front. Neurosci.* **11**, 497 (2017).
- Yuk, H., Lu, B. & Zhao, X. Hydrogel bioelectronics. *Chem. Soc. Rev.* **48**, 1642–1667 (2019).
- Frank, J. A., Antonini, M.-J. & Anikeeva, P. Next-generation interfaces for studying neural function. *Nat. Biotechnol.* **37**, 1013–1023 (2019).
- Kerner, W. Implantable glucose sensors: present status and future developments. *Exp. Clin. Endocrinol. Diabetes* **109**, S341–S346 (2001).
- Moussy, F. in *Proc. IEEE Sensors 2002* vol. 1 270–273 (IEEE, 2002).
- Ward, W. K. A review of the foreign-body response to subcutaneously-implanted devices: the role of macrophages and cytokines in biofouling and fibrosis. *J. Diabetes Sci. Technol.* **2**, 768–777 (2008).
- Farra, R. et al. First-in-human testing of a wirelessly controlled drug delivery microchip. *Sci. Transl. Med.* **4**, 122ra121 (2012).
- Ross, P., Milburn, J., Reith, D., Wiltshire, E. & Wheeler, B. Clinical review: insulin pump-associated adverse events in adults and children. *Acta Diabetol.* **52**, 1017–1024 (2015).
- Heinemann, L. et al. Insulin pump risks and benefits: a clinical appraisal of pump safety standards, adverse event reporting, and research needs: a joint statement of the European Association for the Study of Diabetes and the American Diabetes Association Diabetes Technology Working Group. *Diabetes Care* **38**, 716–722 (2015).
- Rogers, J. A., Someya, T. & Huang, Y. Materials and mechanics for stretchable electronics. *Science* **327**, 1603–1607 (2010).
- Kim, D. H., Xiao, J., Song, J., Huang, Y. & Rogers, J. A. Stretchable, curvilinear electronics based on inorganic materials. *Adv. Mater.* **22**, 2108–2124 (2010).
- Kim, D.-H. et al. Epidermal electronics. *Science* **333**, 838–843 (2011).
- Kim, D.-H., Ghaffari, R., Lu, N. & Rogers, J. A. Flexible and stretchable electronics for biointegrated devices. *Annu. Rev. Biomed. Eng.* **14**, 113–128 (2012).
- Hong, G. & Lieber, C. M. Novel electrode technologies for neural recordings. *Nat. Rev. Neurosci.* **20**, 330–345 (2019).
- Jeong, J. W. et al. Materials and optimized designs for human-machine interfaces via epidermal electronics. *Adv. Mater.* **25**, 6839–6846 (2013).
- Deng, J. et al. Electrical bioadhesive interface for bioelectronics. *Nat. Mater.* **20**, 229–236 (2021).
- Someya, T., Bao, Z. & Malliaras, G. G. The rise of plastic bioelectronics. *Nature* **540**, 379–385 (2016).
- Chen, R., Canales, A. & Anikeeva, P. Neural recording and modulation technologies. *Nat. Rev. Mater.* **2**, 16093 (2017).
- Feiner, R. & Dvir, T. Tissue–electronics interfaces: from implantable devices to engineered tissues. *Nat. Rev. Mater.* **3**, 17076 (2018).
- Anderson, J. M., Rodriguez, A. & Chang, D. T. Foreign body reaction to biomaterials. *Semin. Immunol.* **20**, 86–100 (2008).
- Rolfe, B. et al. in *Regenerative Medicine and Tissue Engineering: Cells and Biomaterials* (ed. Eberli, D.) (IntechOpen, 2011).
- Anderson, J. M. Biological responses to materials. *Annu. Rev. Mater. Res.* **31**, 81–110 (2001).
- Voskerkian, C. et al. Biocompatibility and biofouling of MEMS drug delivery devices. *Biomaterials* **24**, 1959–1967 (2003).
- Wick, G. et al. The immunology of fibrosis. *Annu. Rev. Immunol.* **31**, 107–135 (2013).
- Harding, J. L. & Reynolds, M. M. Combating medical device fouling. *Trends Biotechnol.* **32**, 140–146 (2014).
- Sadtler, K. et al. Design, clinical translation and immunological response of biomaterials in regenerative medicine. *Nat. Rev. Mater.* **1**, 16040 (2016).
- Wichterle, O. & Lim, D. Hydrophilic gels for biological use. *Nature* **185**, 117–118 (1960).
- Lee, K. Y. & Mooney, D. J. Hydrogels for tissue engineering. *Chem. Rev.* **101**, 1869–1880 (2001).
- Peppers, N. A., Hilt, J. Z., Khademhosseini, A. & Langer, R. Hydrogels in biology and medicine: from molecular principles to bionanotechnology. *Adv. Mater.* **18**, 1345–1360 (2006).
- Zhao, X. et al. Soft materials by design: unconventional polymer networks give extreme properties. *Chem. Rev.* **212**, 4309–4372 (2021).
- Calvert, P. Hydrogels for soft machines. *Adv. Mater.* **21**, 743–756 (2009).
- Seliktar, D. Designing cell-compatible hydrogels for biomedical applications. *Science* **336**, 1124–1128 (2012).
- Zhao, X. Multi-scale multi-mechanism design of tough hydrogels: building dissipation into stretchy networks. *Soft Matter* **10**, 672–687 (2014).
- Zhang, Y. S. & Khademhosseini, A. Advances in engineering hydrogels. *Science* **356**, eaaf3627 (2017).
- Demitri, C. et al. Hydrogel based tissue mimicking phantom for in-vitro ultrasound contrast agents studies. *J. Biomed. Mater. Res. B Appl. Biomater.* **87**, 338–345 (2008).
- Kirschner, C. M. & Anseth, K. S. Hydrogels in healthcare: from static to dynamic material microenvironments. *Acta Mater.* **61**, 931–944 (2013).
- Xue, K. et al. Hydrogels as emerging materials for translational biomedicine. *Adv. Ther.* **2**, 1800088 (2019).
- Aswathy, S., Narendrakumar, U. & Manjubala, I. Commercial hydrogels for biomedical applications. *Heliyon* **6**, e03719 (2020).
- Mandal, A., Clegg, J. R., Anselmo, A. C. & Mitragotri, S. Hydrogels in the clinic. *Bioeng. Transl. Med.* **5**, e10158 (2020).
- Alba, N. A., Scabassi, R. J., Sun, M. & Cui, X. T. Novel hydrogel-based preparation-free EEG electrode. *IEEE Trans. Neural Syst. Rehabil. Eng.* **18**, 415–423 (2010).
- Green, R. A., Baek, S., Poole-Warren, L. A. & Martens, P. J. Conducting polymer-hydrogels for medical electrode applications. *Sci. Technol. Adv. Mater.* **11**, 014107 (2010).
- Johnson, M. I. Transcutaneous electrical nerve stimulation (TENS). *eLS* <https://doi.org/10.1002/9780470015902.a0024044> (2012).
- Nagamine, K. et al. Noninvasive sweat-lactate biosensor employing a hydrogel-based touch pad. *Sci. Rep.* **9**, 10102 (2019).
- Zhao, F. et al. Ultra-simple wearable local sweat volume monitoring patch based on swellable hydrogels. *Lab Chip* **20**, 168–174 (2020).

48. Bariya, M., Nyein, H. Y. Y. & Javey, A. Wearable sweat sensors. *Nat. Electron.* **1**, 160–171 (2018).
49. Yao, H., Marcheselli, C., Afanasiev, A., Lähdesmäki, I. & Parviz, B. In *IEEE 25th International Conference on Micro Electro Mechanical Systems (MEMS)* 769–772 (IEEE, 2012).
50. Park, J. et al. Soft, smart contact lenses with integrations of wireless circuits, glucose sensors, and displays. *Sci. Adv.* **4**, eaap9841 (2018).
51. Kim, J. et al. Wearable smart sensor systems integrated on soft contact lenses for wireless ocular diagnostics. *Nat. Commun.* **8**, 14997 (2017).
52. Yin, R. et al. Soft transparent graphene contact lens electrodes for conformal full-cornea recording of electroretinogram. *Nat. Commun.* **9**, 2334 (2018).
53. Mirani, B. et al. An advanced multifunctional hydrogel-based dressing for wound monitoring and drug delivery. *Adv. Healthc. Mater.* **6**, 1700718 (2017).
54. Liu, L. et al. A pH-Indicating colorimetric tough hydrogel patch towards applications in a substrate for smart wound dressings. *Polymers* **9**, 558 (2017).
55. Gianino, E., Miller, C. & Gilmore, J. Smart wound dressings for diabetic chronic wounds. *Bioengineering* **5**, 51 (2018).
56. Blacklow, S. et al. Bioinspired mechanically active adhesive dressings to accelerate wound closure. *Sci. Adv.* **5**, eaaw3963 (2019).
57. Liu, J. et al. Triggerable tough hydrogels for gastric resident dosage forms. *Nat. Commun.* **8**, 124 (2017).
58. Liu, X. et al. Ingestible hydrogel device. *Nat. Commun.* **10**, 493 (2019).
59. Steiger, C. et al. Ingestible electronics for diagnostics and therapy. *Nat. Rev. Mater.* **4**, 83–98 (2019).
60. Freeman, M. E., Furey, M. J., Love, B. J. & Hampton, J. M. Friction, wear, and lubrication of hydrogels as synthetic articular cartilage. *Wear* **241**, 129–135 (2000).
61. Gong, J. P. et al. Synthesis of hydrogels with extremely low surface friction. *J. Am. Chem. Soc.* **123**, 5582–5583 (2001).
62. Kaneko, D., Tada, T., Kurokawa, T., Gong, J. P. & Osada, Y. Mechanically strong hydrogels with ultra-low frictional coefficients. *Adv. Mater.* **17**, 535–538 (2005).
63. Ahmed, J. & Gong, J. P. in *Encyclopedia of Polymeric Nanomaterials* (eds Kobayashi, S. & Müllen, K.) 958–966 (Springer, 2015).
64. Yu, Y. et al. Multifunctional “hydrogel skins” on diverse polymers with arbitrary shapes. *Adv. Mater.* **31**, 1807101 (2019).
65. Lin, W. et al. Cartilage-inspired, lipid-based boundary-lubricated hydrogels. *Science* **370**, 335–338 (2020).
66. Jiang, S. & Cao, Z. Ultralow-fouling, functionalizable, and hydrolyzable zwitterionic materials and their derivatives for biological applications. *Adv. Mater.* **22**, 920–932 (2010).
67. Murosaki, T., Ahmed, N. & Gong, J. P. Antifouling properties of hydrogels. *Sci. Technol. Adv. Mater.* **12**, 064706 (2012).
68. Parada, G. et al. Ultrathin and robust hydrogel coatings on cardiovascular medical devices to mitigate thromboembolic and infectious complications. *Adv. Healthc. Mater.* **9**, 2001116 (2020).
69. Lu, Y. et al. Poly (vinyl alcohol)/poly (acrylic acid) hydrogel coatings for improving electrode–neural tissue interface. *Biomaterials* **30**, 4143–4151 (2009).
70. Zhang, L. et al. Zwitterionic hydrogels implanted in mice resist the foreign-body reaction. *Nat. Biotechnol.* **31**, 553–556 (2013).
71. Vegas, A. J. et al. Combinatorial hydrogel library enables identification of materials that mitigate the foreign body response in primates. *Nat. Biotechnol.* **34**, 345 (2016).
72. Spencer, K. C. et al. Characterization of mechanically matched hydrogel coatings to improve the biocompatibility of neural implants. *Sci. Rep.* **7**, 1952 (2017).
73. Xie, X. et al. Reduction of measurement noise in a continuous glucose monitor by coating the sensor with a zwitterionic polymer. *Nat. Biomed. Eng.* **2**, 894 (2018).
74. Bochenek, M. A. et al. Alginate encapsulation as long-term immune protection of allogeneic pancreatic islet cells transplanted into the omental bursa of macaques. *Nat. Biomed. Eng.* **2**, 810–821 (2018).
75. Zhang, Y. et al. Fundamentals and applications of zwitterionic antifouling polymers. *J. Phys. D* **52**, 403001 (2019).
76. Sheng, H. et al. Neural interfaces by hydrogels. *Extrem. Mech. Lett.* **30**, 100510 (2019).
77. Liu, Y. et al. Soft and elastic hydrogel-based microelectronics for localized low-voltage neuromodulation. *Nat. Biomed. Eng.* **3**, 58–68 (2019).
78. Liu, Y. et al. Morphing electronics enable neuromodulation in growing tissue. *Nat. Biotechnol.* **38**, 1031–1036 (2020).
79. Gaharwar, A. K., Peppas, N. A. & Khademhosseini, A. Nanocomposite hydrogels for biomedical applications. *Biotechnol. Bioeng.* **111**, 441–453 (2014).
80. Webber, M. J., Appel, E. A., Meijer, E. & Langer, R. Supramolecular biomaterials. *Nat. Mater.* **15**, 13–26 (2016).
81. Lu, Y., Aimetti, A. A., Langer, R. & Gu, Z. Bioresponsive materials. *Nat. Rev. Mater.* **2**, 16075 (2016).
82. Chaudhuri, O. et al. Hydrogels with tunable stress relaxation regulate stem cell fate and activity. *Nat. Mater.* **15**, 326–334 (2016).
83. Chaudhuri, O., Cooper-White, J., Janmey, P. A., Mooney, D. J. & Shenoy, V. B. Effects of extracellular matrix viscoelasticity on cellular behaviour. *Nature* **584**, 535–546 (2020).
84. Peppas, N. A. & Khare, A. R. Preparation, structure and diffusional behavior of hydrogels in controlled release. *Adv. Drug Deliv. Rev.* **11**, 1–35 (1993).
85. Gupta, P., Vermani, K. & Garg, S. Hydrogels: from controlled release to pH-responsive drug delivery. *Drug Discov. Today* **7**, 569–579 (2002).
86. Lin, C.-C. & Metters, A. T. Hydrogels in controlled release formulations: network design and mathematical modeling. *Adv. Drug Deliv. Rev.* **58**, 1379–1408 (2006).
87. Li, J. & Mooney, D. J. Designing hydrogels for controlled drug delivery. *Nat. Rev. Mater.* **1**, 16071 (2016).
88. Liu, X., Liu, J., Lin, S. & Zhao, X. Hydrogel machines. *Science* **357**, 102–124 (2020).
89. Johnson, M. Transcutaneous electrical nerve stimulation: mechanisms, clinical application and evidence. *Rev. Pain* **1**, 7–11 (2007).
90. Akhtar, A., Sombeck, J., Boyce, B. & Bretl, T. Controlling sensation intensity for electroactile stimulation in human-machine interfaces. *Sci. Robot.* **3**, eaap9770 (2018).
91. Luna, J. L. V., Krenn, M., Cortés Ramirez, J. A. & Mayr, W. Dynamic impedance model of the skin-electrode interface for transcutaneous electrical stimulation. *PLoS ONE* **10**, e0130368 (2015).
92. Yang, C. & Suo, Z. Hydrogel ionotronics. *Nat. Rev. Mater.* **3**, 125 (2018).
93. Prokop, A. F. et al. Polyacrylamide gel as an acoustic coupling medium for focused ultrasound therapy. *Ultrasound Med. Biol.* **29**, 1351–1358 (2003).
94. Zell, K., Sperl, J. I., Vogel, M. W., Niessner, R. & Haisch, C. Acoustical properties of selected tissue phantom materials for ultrasound imaging. *Phys. Med. Biol.* **52**, N475 (2007).
95. Casarotto, R. A., Adamowski, J. C., Fallopa, F. & Bacanelli, F. Coupling agents in therapeutic ultrasound: acoustic and thermal behavior. *Arch. Phys. Med. Rehabil.* **85**, 162–165 (2004).
96. Miller, D. L. et al. Overview of therapeutic ultrasound applications and safety considerations. *J. Ultrasound Med.* **31**, 623–634 (2012).
97. Boateng, J. S., Matthews, K. H., Stevens, H. N. & Eccleston, G. M. Wound healing dressings and drug delivery systems: a review. *J. Pharm. Sci.* **97**, 2892–2923 (2008).
98. Hamed, H., Moradi, S., Hudson, S. M. & Tonelli, A. E. Chitosan based hydrogels and their applications for drug delivery in wound dressings: a review. *Carbohydr. Polym.* **199**, 445–460 (2018).
99. Caló, E. & Khutoryanskiy, V. V. Biomedical applications of hydrogels: a review of patents and commercial products. *Eur. Polym. J.* **65**, 252–267 (2015).
100. Tricoli, A., Nasiri, N. & De, S. Wearable and miniaturized sensor technologies for personalized and preventive medicine. *Adv. Funct. Mater.* **27**, 1605271 (2017).
101. Lee, H. et al. A graphene-based electrochemical device with thermoresponsive microneedles for diabetes monitoring and therapy. *Nat. Nanotechnol.* **11**, 566 (2016).
102. Koh, A. et al. A soft, wearable microfluidic device for the capture, storage, and colorimetric sensing of sweat. *Sci. Transl. Med.* **8**, 366ra165 (2016).
103. Gao, W. et al. Fully integrated wearable sensor arrays for multiplexed in situ perspiration analysis. *Nature* **529**, 509–514 (2016).
104. Wang, C. et al. Monitoring of the central blood pressure waveform via a conformal ultrasonic device. *Nat. Biomed. Eng.* **2**, 687 (2018).
105. Chung, H. U. et al. Binodal, wireless epidermal electronic systems with in-sensor analytics for neonatal intensive care. *Science* **363**, eaau0780 (2019).
106. Kim, J., Campbell, A. S., de Ávila, B. E.-F. & Wang, J. Wearable biosensors for healthcare monitoring. *Nat. Biotechnol.* **37**, 389–406 (2019).
107. Chung, H. U. et al. Skin-interfaced biosensors for advanced wireless physiological monitoring in neonatal and pediatric intensive-care units. *Nat. Med.* **26**, 418–429 (2020).
108. Stapleton, F., Stretton, S., Pappas, E., Skotnitsky, C. & Sweeney, D. F. Silicone hydrogel contact lenses and the ocular surface. *Ocul. Surf.* **4**, 24–45 (2006).
109. Kirchhof, S., Goepferich, A. M. & Brandl, F. P. Hydrogels in ophthalmic applications. *Eur. J. Pharm. Biopharm.* **95**, 227–238 (2015).
110. Lee, G.-H. et al. Multifunctional materials for implantable and wearable photonic healthcare devices. *Nat. Rev. Mater.* **5**, 149–165 (2020).
111. Lloyd, J. D., Marque, M. J. III & Kacprowicz, R. F. Closure techniques. *Emerg. Med. Clin. North Am.* **25**, 73–81 (2007).
112. Slieker, J. C., Daams, F., Mulder, I. M., Jeekel, J. & Lange, J. F. Systematic review of the technique of colorectal anastomosis. *JAMA Surg.* **148**, 190–201 (2013).
113. Annabi, N., Yue, K., Tamayol, A. & Khademhosseini, A. Elastic sealants for surgical applications. *Eur. J. Pharm. Biopharm.* **95**, 27–39 (2015).
114. Munoz Taboada, G. et al. Overcoming the translational barriers of tissue adhesives. *Nat. Rev. Mater.* **5**, 310–329 (2020).
115. Nam, S. & Mooney, D. Polymeric tissue adhesives. *Chem. Rev.* **121**, 11336–11384 (2021).
116. Li, J. et al. Tough adhesives for diverse wet surfaces. *Science* **357**, 378–381 (2017).
117. Yuk, H. et al. Dry double-sided tape for adhesion of wet tissues and devices. *Nature* **575**, 169–174 (2019).
118. Sharma, B. et al. Human cartilage repair with a photoreactive adhesive-hydrogel composite. *Sci. Transl. Med.* **5**, 167ra166 (2013).
119. Annabi, N. et al. Engineering a highly elastic human protein–based sealant for surgical applications. *Sci. Transl. Med.* **9**, eaai7466 (2017).
120. Okun, M. S. Deep-brain stimulation for Parkinson’s disease. *N. Engl. J. Med.* **367**, 1529–1538 (2012).
121. Hickey, P. & Stacy, M. Deep brain stimulation: a paradigm shifting approach to treat Parkinson’s disease. *Front. Neurosci.* **10**, 173 (2016).
122. Fox, D. The electric cure. *Nature* **545**, 20–22 (2017).
123. Mineev, I. R. et al. Electronic dura mater for long-term multimodal neural interfaces. *Science* **347**, 159–163 (2015).
124. Wenger, N. et al. Spatiotemporal neuromodulation therapies engaging muscle synergies improve motor control after spinal cord injury. *Nat. Med.* **22**, 138 (2016).
125. Formento, E. et al. Electrical spinal cord stimulation must preserve proprioception to enable locomotion in humans with spinal cord injury. *Nat. Neurosci.* **21**, 1728–1741 (2018).
126. Wagner, F. B. et al. Targeted neurotechnology restores walking in humans with spinal cord injury. *Nature* **563**, 65–71 (2018).
127. Courtine, G. & Sofroniew, M. V. Spinal cord repair: advances in biology and technology. *Nat. Med.* **25**, 898–908 (2019).
128. Park, J. et al. Electromechanical cardioplasty using a wrapped elasto-conductive epicardial mesh. *Sci. Transl. Med.* **8**, 344ra386 (2016).
129. Freedman, B. et al. Management of atrial high-rate episodes detected by cardiac implanted electronic devices. *Nat. Rev. Cardiol.* **14**, 701–714 (2017).
130. Cingolani, E., Goldhaber, J. I. & Marbán, E. Next-generation pacemakers: from small devices to biological pacemakers. *Nat. Rev. Cardiol.* **15**, 139–150 (2018).
131. Yacoub, M. H. & McLeod, C. The expanding role of implantable devices to monitor heart failure and pulmonary hypertension. *Nat. Rev. Cardiol.* **15**, 770–779 (2018).
132. Dhanasingh, A. & Jolly, C. An overview of cochlear implant electrode array designs. *Hear. Res.* **356**, 93–103 (2017).
133. Ortiz-Catalan, M., Håkansson, B. & Brånemark, R. An osseointegrated human-machine gateway for long-term sensory feedback and motor control of artificial limbs. *Sci. Transl. Med.* **6**, 257re256 (2014).
134. Farina, D. et al. Man/machine interface based on the discharge timings of spinal motor neurons after



- targeted muscle reinnervation. *Nat. Biomed. Eng.* **1**, 0025 (2017).
135. Ortiz-Catalan, M., Mastinu, E., Sassu, P., Aszmann, O. & Brånemark, R. Self-contained neuromusculoskeletal arm prostheses. *N. Engl. J. Med.* **382**, 1732–1738 (2020).
136. Rao, L., Zhou, H., Li, T., Li, C. & Duan, Y. Y. Polyethylene glycol-containing polyurethane hydrogel coatings for improving the biocompatibility of neural electrodes. *Acta Biomater.* **8**, 2233–2242 (2012).
137. Aregueta-Robles, U. A., Woolley, A. J., Poole-Warren, L. A., Lovell, N. H. & Green, R. A. Organic electrode coatings for next-generation neural interfaces. *Front. Neuroeng.* **7**, 15 (2014).
138. Yuk, H. et al. 3D printing of conducting polymers. *Nat. Commun.* **11**, 1604 (2020).
139. Inoue, A., Yuk, H., Lu, B. & Zhao, X. Strong adhesion of wet conducting polymers on diverse substrates. *Sci. Adv.* **6**, eaay5394 (2020).
140. Sahel, J.-A. et al. Partial recovery of visual function in a blind patient after optogenetic therapy. *Nat. Med.* **27**, 1223–1229 (2021).
141. Choi, M. et al. Light-guiding hydrogels for cell-based sensing and optogenetic synthesis in vivo. *Nat. Photonics* **7**, 987 (2013).
142. Guo, J. et al. Highly stretchable, strain sensing hydrogel optical fibers. *Adv. Mater.* **28**, 10244–10249 (2016).
143. Nazempour, R., Zhang, Q., Fu, R. & Sheng, X. Biocompatible and implantable optical fibers and waveguides for biomedicine. *Materials* **11**, 1283 (2018).
144. Guo, J., Yang, C., Dai, Q. & Kong, L. Soft and stretchable polymeric optical waveguide-based sensors for wearable and biomedical applications. *Sensors* **19**, 3771 (2019).
145. Langer, R. Drug delivery and targeting. *Nature* **392**, 5–10 (1998).
146. Peppas, N. A. & Van Blarcom, D. S. Hydrogel-based biosensors and sensing devices for drug delivery. *J. Control. Release* **240**, 142–150 (2016).
147. Bjugstad, K., Lampe, K., Kern, D. & Mahoney, M. Biocompatibility of poly(ethylene glycol)-based hydrogels in the brain: an analysis of the glial response across space and time. *J. Biomed. Mater. Res. A* **95**, 79–91 (2010).
148. Mack, M. J. Minimally invasive and robotic surgery. *JAMA* **285**, 568–572 (2001).
149. Liu, X. et al. Magnetic living hydrogels for intestinal localization, retention, and diagnosis. *Adv. Funct. Mater.* **31**, 2010918 (2021).
150. Greenway, F. L. et al. A randomized, double-blind, placebo-controlled study of Gelesis100: a novel nonsystemic oral hydrogel for weight loss. *Obesity* **27**, 205–216 (2019).
151. Deem, M. E. Guidewire having hydrophilic coating. US Patent 5,840,046 (1998).
152. Bologna, R. A., Polansky, M., Framow, H. D., Gordon, D. A. & Whitmore, K. E. Hydrogel/silver ion-coated urinary catheter reduces nosocomial urinary tract infection rates in intensive care unit patients: a multicenter study. *Urology* **54**, 982–987 (1999).
153. Lederer, J. W., Jarvis, W. R., Thomas, L. & Ritter, J. Multicenter cohort study to assess the impact of a silver-alloy and hydrogel-coated urinary catheter on symptomatic catheter-associated urinary tract infections. *J. Wound Ostomy Cont. Nurs.* **41**, 473 (2014).
154. Kim, Y., Parada, G. A., Liu, S. & Zhao, X. Ferromagnetic soft continuum robots. *Sci. Robot.* **4**, eaax7329 (2019).
155. John, T., Rajpurkar, A., Smith, G., Fairfax, M. & Triest, J. Antibiotic pretreatment of hydrogel ureteral stent. *J. Endourol.* **21**, 1211–1216 (2007).
156. Obiteluozor, F. O. et al. Thromboresistant semi-IPN hydrogel coating: towards improvement of the hemocompatibility/biocompatibility of metallic stent implants. *Mater. Sci. Eng. C* **99**, 1274–1288 (2019).
157. Lopes, P. A. et al. Soft bioelectronic stickers: selection and evaluation of skin-interfacing electrodes. *Adv. Healthc. Mater.* **8**, 1900234 (2019).
158. Gong, J. P., Katsuyama, Y., Kurokawa, T. & Osada, Y. Double-network hydrogels with extremely high mechanical strength. *Adv. Mater.* **15**, 1155–1158 (2003).
159. Sun, J.-Y. et al. Highly stretchable and tough hydrogels. *Nature* **489**, 133–136 (2012).
160. Wang, Q., Hou, R., Cheng, Y. & Fu, J. Super-tough double-network hydrogels reinforced by covalently compositing with silica-nanoparticles. *Soft Matter* **8**, 6048–6056 (2012).
161. Liu, R. et al. Tough and highly stretchable graphene oxide/polyacrylamide nanocomposite hydrogels. *J. Mater. Chem.* **22**, 14160–14167 (2012).
162. Yuk, H., Zhang, T., Lin, S., Parada, G. A. & Zhao, X. Tough bonding of hydrogels to diverse non-porous surfaces. *Nat. Mater.* **15**, 190–196 (2016).
163. Yuk, H., Zhang, T., Parada, G. A., Liu, X. & Zhao, X. Skin-inspired hydrogel–elastomer hybrids with robust interfaces and functional microstructures. *Nat. Commun.* **7**, 12028 (2016).
164. Yang, J., Bai, R. & Suo, Z. Topological adhesion of wet materials. *Adv. Mater.* **30**, 1800671 (2018).
165. Yang, S. Y. et al. A bio-inspired swellable microneedle adhesive for mechanical interlocking with tissue. *Nat. Commun.* **4**, 1702 (2013).
166. Liu, J. et al. Fatigue-resistant adhesion of hydrogels. *Nat. Commun.* **11**, 1071 (2020).
167. Huebsch, N. et al. Ultrasound-triggered disruption and self-healing of reversibly cross-linked hydrogels for drug delivery and enhanced chemotherapy. *Proc. Natl Acad. Sci. USA* **111**, 9762–9767 (2014).
168. Schoellhammer, C. M. et al. Ultrasound-mediated gastrointestinal drug delivery. *Sci. Transl. Med.* **7**, 310ra168 (2015).
169. Chen, L. et al. Soft elastic hydrogel couplants for ultrasonography. *Mater. Sci. Eng. C* **119**, 111609 (2021).
170. Corvino, A. et al. Utility of a gel stand-off pad in the detection of Doppler signal on focal nodular lesions of the skin. *J. Ultrasound* **23**, 45–53 (2020).
171. Gabriel, C., Peyman, A. & Grant, E. H. Electrical conductivity of tissue at frequencies below 1 MHz. *Phys. Med. Biol.* **54**, 4863 (2009).
172. Cogan, S. F. Neural stimulation and recording electrodes. *Annu. Rev. Biomed. Eng.* **10**, 275–309 (2008).
173. Rivnay, J., Wang, H., Fenko, L., Deisseroth, K. & Malliaras, G. G. Next-generation probes, particles, and proteins for neural interfacing. *Sci. Adv.* **3**, e1601649 (2017).
174. Choi, M., Humar, M., Kim, S. & Yun, S. H. Step-index optical fiber made of biocompatible hydrogels. *Adv. Mater.* **27**, 4081–4086 (2015).
175. Ehrbar, M., Schoenmakers, R., Christen, E. H., Fussenegger, M. & Weber, W. Drug-sensing hydrogels for the inducible release of biopharmaceuticals. *Nat. Mater.* **7**, 800–804 (2008).
176. Hendrickson, G. R. & Lyon, L. A. Bioresponsive hydrogels for sensing applications. *Soft Matter* **5**, 29–35 (2009).
177. Buenger, D., Topuz, F. & Groll, J. Hydrogels in sensing applications. *Prog. Polym. Sci.* **37**, 1678–1719 (2012).
178. Elshaarani, T. et al. Synthesis of hydrogel-bearing phenylboronic acid moieties and their applications in glucose sensing and insulin delivery. *J. Mater. Chem. B* **6**, 3831–3854 (2018).
179. Sinha, A. et al. Polymer hydrogel interfaces in electrochemical sensing strategies: a review. *TrAC. Trends Anal. Chem.* **118**, 488–501 (2019).
180. Dee, K. C., Puleo, D. A. & Bizios, R. *An Introduction to Tissue-Biomaterial Interactions* (Wiley, 2003).
181. Li, C. et al. Design of biodegradable, implantable devices towards clinical translation. *Nat. Rev. Mater.* **5**, 61–81 (2019).
182. Green, J. J. & Elisseeff, J. H. Mimicking biological functionality with polymers for biomedical applications. *Nature* **540**, 386–394 (2016).
183. Davidson, M. D., Burdick, J. A. & Wells, R. G. Engineered biomaterial platforms to study fibrosis. *Adv. Healthc. Mater.* **9**, 1901682 (2020).
184. Fattahi, P., Yang, G., Kim, G. & Abidian, M. R. A review of organic and inorganic biomaterials for neural interfaces. *Adv. Mater.* **26**, 1846–1885 (2014).
185. Morais, J. M., Papadimitrakopoulos, F. & Burgess, D. J. Biomaterials/tissue interactions: possible solutions to overcome foreign body response. *AAPS J.* **12**, 188–196 (2010).
186. Koh, A., Nichols, S. P. & Schoenfish, M. H. Glucose sensor membranes for mitigating the foreign body response. *J. Diabetes Sci. Technol.* **5**, 1052–1059 (2011).
187. Arciola, C. R., Campoccia, D. & Montanaro, L. Implant infections: adhesion, biofilm formation and immune evasion. *Nat. Rev. Microbiol.* **16**, 397 (2018).
188. Zhang, D. et al. Dealing with the foreign-body response to implanted biomaterials: strategies and applications of new materials. *Adv. Funct. Mater.* **31**, 2007226 (2020).
189. Nichol, J. W. et al. Cell-laden microengineered gelatin methacrylate hydrogels. *Biomaterials* **31**, 5536–5544 (2010).
190. Yue, K. et al. Synthesis, properties, and biomedical applications of gelatin methacryloyl (GelMA) hydrogels. *Biomaterials* **73**, 254–271 (2015).
191. Augst, A. D., Kong, H. J. & Mooney, D. J. Alginate hydrogels as biomaterials. *Macromol. Biosci.* **6**, 623–635 (2006).
192. Lee, K. Y. & Mooney, D. J. Alginate: properties and biomedical applications. *Prog. Polym. Sci.* **37**, 106–126 (2012).
193. Rowley, J. A., Madlambayan, G. & Mooney, D. J. Alginate hydrogels as synthetic extracellular matrix materials. *Biomaterials* **20**, 45–53 (1999).
194. Berger, J. et al. Structure and interactions in covalently and ionically crosslinked chitosan hydrogels for biomedical applications. *Eur. J. Pharm. Biopharm.* **57**, 19–34 (2004).
195. Ahmadi, F., Oveis, Z., Samani, S. M. & Amoozgar, Z. Chitosan based hydrogels: characteristics and pharmaceutical applications. *Res. Pharm. Sci.* **10**, 1–16 (2015).
196. Pellá, M. C. et al. Chitosan-based hydrogels: from preparation to biomedical applications. *Carbohydr. Polym.* **196**, 233–245 (2018).
197. Wang, Z. et al. Functional regeneration of tendons using scaffolds with physical anisotropy engineered via microarchitectural manipulation. *Sci. Adv.* **4**, eaat4537 (2018).
198. Yang, G., Lin, H., Rothrauff, B. B., Yu, S. & Tuan, R. S. Multilayered polycaprolactone/gelatin fiber-hydrogel composite for tendon tissue engineering. *Acta Biomater.* **35**, 68–76 (2016).
199. Mredha, M. T. I. et al. A facile method to fabricate anisotropic hydrogels with perfectly aligned hierarchical fibrous structures. *Adv. Mater.* **30**, 1704937 (2018).
200. Lin, S., Liu, J., Liu, X. & Zhao, X. Muscle-like fatigue-resistant hydrogels by mechanical training. *Proc. Natl Acad. Sci. USA* **116**, 10244–10249 (2019).
201. Hua, M. et al. Strong tough hydrogels via the synergy of freeze-drying and salting out. *Nature* **590**, 594–599 (2021).
202. Rossetti, L. et al. The microstructure and micromechanics of the tendon–bone insertion. *Nat. Mater.* **16**, 664–670 (2017).
203. Nonoyama, T. et al. Double-network hydrogels strongly bondable to bones by spontaneous osteogenesis penetration. *Adv. Mater.* **28**, 6740–6745 (2016).
204. Rauner, N., Meuris, M., Zoric, M. & Tiller, J. C. Enzymatic mineralization generates ultrastiff and tough hydrogels with tunable mechanics. *Nature* **543**, 407–410 (2017).
205. Discher, D. E., Janmey, P. & Wang, Y.-L. Tissue cells feel and respond to the stiffness of their substrate. *Science* **310**, 1139–1143 (2005).
206. Lin, X. et al. A viscoelastic adhesive epicardial patch for treating myocardial infarction. *Nat. Biomed. Eng.* **3**, 632–643 (2019).
207. Tringides, C. M. et al. Viscoelastic surface electrode arrays to interface with viscoelastic tissues. *Nat. Nanotechnol.* **5**, 1019–1029 (2021).
208. Gong, J. P. Why are double network hydrogels so tough? *Soft Matter* **6**, 2583–2590 (2010).
209. Zhang, T., Yuk, H., Lin, S., Parada, G. A. & Zhao, X. Tough and tunable adhesion of hydrogels: experiments and models. *Acta Mech. Sin.* **33**, 543–554 (2017).
210. Chen, X., Yuk, H., Wu, J., Nabzdyk, C. S. & Zhao, X. Instant tough bioadhesive with triggerable benign detachment. *Proc. Natl Acad. Sci. USA* **117**, 15497–15503 (2020).
211. Chen, J. et al. An adhesive hydrogel with “load-sharing” effect as tissue bandages for drug and cell delivery. *Adv. Mater.* **32**, 2001628 (2020).
212. Gong, J. P. Friction and lubrication of hydrogels — its richness and complexity. *Soft Matter* **2**, 544–552 (2006).
213. Mu, R. et al. Polymer-filled macroporous hydrogel for low friction. *Extrem. Mech. Lett.* **38**, 100742 (2020).
214. Skudrzyk, E. *The Foundations of Acoustics: Basic Mathematics and Basic Acoustics* (Springer, 2012).
215. Yuk, H. et al. Hydraulic hydrogel actuators and robots optically and sonically camouflaged in water. *Nat. Commun.* **8**, 14230 (2017).
216. Lee, W., Lee, S. D., Park, M. Y., Yang, J. & Yoo, S. S. Evaluation of polyvinyl alcohol cryogel as an acoustic coupling medium for low-intensity transcranial focused ultrasound. *Int. J. Imaging Syst. Technol.* **24**, 332–338 (2014).
217. Dvir, T. et al. Nanowired three-dimensional cardiac patches. *Nat. Nanotechnol.* **6**, 720–725 (2011).
218. Ahn, Y., Lee, H., Lee, D. & Lee, Y. Highly conductive and flexible silver nanowire-based microelectrodes on biocompatible hydrogel. *ACS Appl. Mater. Interfaces* **6**, 18401–18407 (2014).
219. Shin, S. R. et al. Carbon-nanotube-embedded hydrogel sheets for engineering cardiac constructs and bioactuators. *ACS Nano* **7**, 2369–2380 (2013).
220. Song, H. S., Kwon, O. S., Kim, J.-H., Conde, J. & Artzi, N. 3D hydrogel scaffold doped with 2D graphene materials

- for biosensors and bioelectronics. *Biosens. Bioelectron.* **89**, 187–200 (2017).
221. Pan, L. et al. Hierarchical nanostructured conducting polymer hydrogel with high electrochemical activity. *Proc. Natl Acad. Sci. USA* **109**, 9287–9292 (2012).
  222. Yao, B. et al. Ultrahigh-conductivity polymer hydrogels with arbitrary structures. *Adv. Mater.* **29**, 1700974 (2017).
  223. Lu, B. et al. Pure PEDOT: PSS hydrogels. *Nat. Commun.* **10**, 1043 (2019).
  224. Proctor, C. M., Rivnay, J. & Malliaras, G. G. Understanding volumetric capacitance in conducting polymers. *J. Polym. Sci. B Polym. Phys.* **54**, 1433–1436 (2016).
  225. Paulsen, B. D., Tybrandt, K., Stavrinidou, E. & Rivnay, J. Organic mixed ionic–electronic conductors. *Nat. Mater.* **19**, 13–26 (2020).
  226. Zhang, Q. et al. High refractive index inorganic–organic interpenetrating polymer network (IPN) hydrogel nanocomposite toward artificial cornea implants. *ACS Macro Lett.* **1**, 876–881 (2012).
  227. Tummala, G. K., Joffre, T., Rojas, R., Persson, C. & Mhuran, A. Strain-induced stiffening of nanocellulose-reinforced poly (vinyl alcohol) hydrogels mimicking collagenous soft tissues. *Soft Matter* **13**, 3936–3945 (2017).
  228. Ritger, P. L. & Peppas, N. A. A simple equation for description of solute release I. Fickian and non-fickian release from non-swellable devices in the form of slabs, spheres, cylinders or discs. *J. Control. Release* **5**, 23–36 (1987).
  229. Ritger, P. L. & Peppas, N. A. A simple equation for description of solute release II. Fickian and anomalous release from swellable devices. *J. Control. Release* **5**, 37–42 (1987).
  230. Cukier, R. Diffusion of Brownian spheres in semidilute polymer solutions. *Macromolecules* **17**, 252–255 (1984).
  231. Deen, W. Hindered transport of large molecules in liquid-filled pores. *AIChE J.* **33**, 1409–1425 (1987).
  232. Amsden, B. Solute diffusion within hydrogels. Mechanisms and models. *Macromolecules* **31**, 8382–8395 (1998).
  233. Esfand, R. & Tomalia, D. A. Poly (amidoamine) (PAMAM) dendrimers: from biomimicry to drug delivery and biomedical applications. *Drug Discov. Today* **6**, 427–436 (2001).
  234. Omidian, H., Rocca, J. G. & Park, K. Advances in superporous hydrogels. *J. Control. Release* **102**, 3–12 (2005).
  235. Zhao, X. et al. Active scaffolds for on-demand drug and cell delivery. *Proc. Natl Acad. Sci. USA* **108**, 67–72 (2011).
  236. Coughlan, D. & Corrigan, O. Drug–polymer interactions and their effect on thermoresponsive poly (N-isopropylacrylamide) drug delivery systems. *Int. J. Pharm.* **313**, 163–174 (2006).
  237. Muir, V. G. & Burdick, J. A. Chemically modified biopolymers for the formation of biomedical hydrogels. *Chem. Rev.* **121**, 10949 (2020).
  238. Correa, S. et al. Translational applications of hydrogels. *Chem. Rev.* **121**, 11385–11457 (2021).
  239. Bouhadir, K. H. et al. Degradation of partially oxidized alginate and its potential application for tissue engineering. *Biotechnol. Prog.* **17**, 945–950 (2001).
  240. Boonthekul, T., Kong, H.-J. & Mooney, D. J. Controlling alginate gel degradation utilizing partial oxidation and bimodal molecular weight distribution. *Biomaterials* **26**, 2455–2465 (2005).
  241. Lin, C.-C. & Anseth, K. S. PEG hydrogels for the controlled release of biomolecules in regenerative medicine. *Pharm. Res.* **26**, 631–643 (2009).
  242. Zustiak, S. P. & Leach, J. B. Hydrolytically degradable poly (ethylene glycol) hydrogel scaffolds with tunable degradation and mechanical properties. *Biomacromolecules* **11**, 1348–1357 (2010).
  243. Burdick, J. A. & Prestwich, G. D. Hyaluronic acid hydrogels for biomedical applications. *Adv. Mater.* **23**, H41–H56 (2011).
  244. Tavakoli, J. & Tang, Y. Hydrogel based sensors for biomedical applications: an updated review. *Polymers* **9**, 364 (2017).
  245. Kim, H., Cohen, R. E., Hammond, P. T. & Irvine, D. J. Live lymphocyte arrays for biosensing. *Adv. Funct. Mater.* **16**, 1313–1323 (2006).
  246. Ulijn, R. V. et al. Bioresponsive hydrogels. *Mater. Today* **10**, 40–48 (2007).
  247. Shibata, H. et al. Injectable hydrogel microbeads for fluorescence-based in vivo continuous glucose monitoring. *Proc. Natl Acad. Sci. USA* **107**, 17894–17898 (2010).
  248. Bhattacharya, S., Sarkar, R., Nandi, S., Porgador, A. & Jelinek, R. Detection of reactive oxygen species by a carbon-dot–ascorbic acid hydrogel. *Anal. Chem.* **89**, 830–836 (2017).
  249. Hynes, R. O. Integrins: versatility, modulation, and signaling in cell adhesion. *Cell* **69**, 11–25 (1992).
  250. Nuttelman, C. R., Mortisen, D. J., Henry, S. M. & Anseth, K. S. Attachment of fibronectin to poly (vinyl alcohol) hydrogels promotes NIH3T3 cell adhesion, proliferation, and migration. *J. Biomed. Mater. Res.* **57**, 217–223 (2001).
  251. Mosahebi, A., Wiberg, M. & Terenghi, G. Addition of fibronectin to alginate matrix improves peripheral nerve regeneration in tissue-engineered conduits. *Tissue Eng.* **9**, 209–218 (2003).
  252. Burdick, J. A. & Anseth, K. S. Photoencapsulation of osteoblasts in injectable RGD-modified PEG hydrogels for bone tissue engineering. *Biomaterials* **23**, 4315–4323 (2002).
  253. Yang, F. et al. The effect of incorporating RGD adhesive peptide in polyethylene glycol diacrylate hydrogel on osteogenesis of bone marrow stromal cells. *Biomaterials* **26**, 5991–5998 (2005).
  254. Chen, S., Li, L., Zhao, C. & Zheng, J. Surface hydration: principles and applications toward low-fouling/nonfouling biomaterials. *Polymer* **51**, 5283–5293 (2010).
  255. Li, J. & Kao, W. J. Synthesis of polyethylene glycol (PEG) derivatives and PEGylated–peptide biopolymer conjugates. *Biomacromolecules* **4**, 1055–1067 (2003).
  256. Costa, F., Carvalho, I. F., Montelaro, R. C., Gomes, P. & Martins, M. C. L. Covalent immobilization of antimicrobial peptides (AMPs) onto biomaterial surfaces. *Acta Biomater.* **7**, 1431–1440 (2011).
  257. Bazaka, K., Jacob, M. V., Crawford, R. J. & Ivanova, E. P. Efficient surface modification of biomaterial to prevent biofilm formation and the attachment of microorganisms. *Appl. Microbiol. Biotechnol.* **95**, 299–311 (2012).
  258. Farah, S. et al. Long-term implant fibrosis prevention in rodents and non-human primates using crystallized drug formulations. *Nat. Mater.* **18**, 892–904 (2019).
  259. Zhu, J. & Marchant, R. E. Design properties of hydrogel tissue-engineering scaffolds. *Expert Rev. Med. Devic.* **8**, 607–626 (2011).
  260. Cho, Y. W. et al. Gentamicin-releasing urethral catheter for short-term catheterization. *J. Biomater. Sci. Polym. Ed.* **14**, 963–972 (2003).
  261. Oxley, T. J. et al. Minimally invasive endovascular stent-electrode array for high-fidelity, chronic recordings of cortical neural activity. *Nat. Biotechnol.* **34**, 320–327 (2016).
  262. Kim, K. O., Kim, G. J. & Kim, J. H. A cellulose/ $\beta$ -cyclodextrin nanofiber patch as a wearable epidermal glucose sensor. *RSC Adv.* **9**, 22790–22794 (2019).
  263. Kim, G. J. & Kim, K. O. Novel glucose-responsive of the transparent nanofiber hydrogel patches as a wearable biosensor via electrospinning. *Sci. Rep.* **10**, 18858 (2020).
  264. Wang, D.-A. et al. Multifunctional chondroitin sulphate for cartilage tissue–biomaterial integration. *Nat. Mater.* **6**, 385–392 (2007).
  265. Foyt, D. A., Norman, M. D., Yu, T. T. & Gentleman, E. Exploiting advanced hydrogel technologies to address key challenges in regenerative medicine. *Adv. Healthc. Mater.* **7**, 1700939 (2018).
  266. Quinn, C. A., Connor, R. E. & Heller, A. Biocompatible, glucose-permeable hydrogel for in situ coating of implantable biosensors. *Biomaterials* **18**, 1665–1670 (1997).
  267. Yetisen, A. K. et al. Glucose-sensitive hydrogel optical fibers functionalized with phenylboronic acid. *Adv. Mater.* **29**, 1606380 (2017).
  268. Kahan, S. & Kumbhari, V. A weight loss device that looks like a pill. *Obesity* **27**, 189–189 (2019).
  269. Kharkar, P. M., Kiick, K. L. & Kloxin, A. M. Designing degradable hydrogels for orthogonal control of cell microenvironments. *Chem. Soc. Rev.* **42**, 7335–7372 (2013).
  270. Edelman, I. & Leibman, J. Anatomy of body water and electrolytes. *Am. J. Med.* **27**, 256–277 (1959).

### Acknowledgements

This work is supported by the National Institute of Health (1-R01-HL153857) and the National Science Foundation (EFMA-1935291). This work is additionally supported by the National Research Foundation, the Prime Minister's Office, Singapore, under its Campus for Research Excellence and Technological Enterprise programme, through the Singapore MIT Alliance for Research and Technology: Critical Analytics for Manufacturing Personalized-Medicine Inter-Disciplinary Research Group. H.Y. acknowledges financial support from Samsung Scholarship. X.Z. acknowledges the George N. Hatsopoulos (1949) Faculty Fellowship from the Massachusetts Institute of Technology and the Humboldt Research Award.

### Author contributions

All authors contributed to the planning, discussion and writing of the manuscript.

### Competing interests

The authors declare no competing interests.

### Peer review information

*Nature Reviews Materials* thanks the anonymous reviewers for their contribution to the peer review of this work.

### Publisher's note

Springer Nature remains neutral with regard to jurisdictional claims in published maps and institutional affiliations.

Springer Nature or its licensor holds exclusive rights to this article under a publishing agreement with the author(s) or other rightsholder(s); author self-archiving of the accepted manuscript version of this article is solely governed by the terms of such publishing agreement and applicable law.

© Springer Nature Limited 2022